energies

MDPI

Review

Reactivity Effects of Inorganic Content in Biomass Gasification: A Review

Anna Trubetskaya

Department of Engineering, University of Limerick, Castletroy, V94 T9PX Limerick, Ireland; anna.trubetskaya@ul.ie

Abstract: This review article discusses the effects of inorganic content and mechanisms on raw biomass and char during gasification. The impacts of the inherent inorganics and externally added inorganic compounds are summarized based on a literature search from the most recent 40 years. The TGA and larger-scale studies involving K-, Ca-, and Si-related mechanisms are critically reviewed with the aim of understanding the reaction mechanisms and kinetics. Differences between the reaction pathways of inorganic matter, and subsequent effects on the reactivity during gasification, are discussed. The present results illustrate the complexity of ash transformation phenomena, which have a strong impact on the design of gasifiers as well as further operation and process control. The impregnation and mixing of catalytic compounds into raw biomass are emphasized as a potential solution to avoid reactivity-related operational challenges during steam and CO_2 gasification. This review clearly identifies a gap in experimental knowledge at the micro and macro levels in the advanced modelling of inorganics transformation with respect to gasification reactivity.

Keywords: inorganic content; biomass; gasification; reactivity; AAEM

Citation: Trubetskaya, A. Reactivity Effects of Inorganic Content in Biomass Gasification: A Review. *Energies* **2022**, *15*, 3137. https://doi.org/10.3390/en15093137

Academic Editors: Dimitrios Sidiras and Leonidas Matsakas

Received: 16 March 2022
Accepted: 21 April 2022
Published: 25 April 2022

1. Introduction

The primary measures for achieving the ambitious targets set by the Paris agreement include carbon capture, storage, and utilization, energy conservation and efficiency improvement, an increased use of renewable resources, and the use of negative emissions technologies (NETs) [1,2]. Bioenergy with carbon capture and storage (BECCS) is looked upon as one of the most promising NETs in spite of some debates over concerns about the timing of CO_2 capture and release. The main reasons for this include the renewable nature and widespread availability of biomass, by contrast with fossil fuels, and the advancing thermochemical and biochemical conversion processes to convert it into biofuels and bioproducts. Thermochemical processes such as gasification and pyrolysis are receiving more attention because of their feedstock flexibility and multi-dimensional applications [3]. The term 'biomass' covers a broad range of organic matter, with lignocellulosic biomass (e.g., wood, energy crops, and agricultural residues) mainly composed of cellulose, hemicellulose, and lignin, as well as ash and extractives. Residual biomass such as low-grade plants, agricultural and forest residues, algae, and municipal solid waste do not compete with food in providing biomass and may serve as the prime feedstocks for thermochemical conversion processes such as pyrolysis and gasification.

For both pyrolysis and gasification, several experimental and modelling studies have investigated the influence of biomass composition and operating parameters on the process performance, as identified by a series of review articles in the last couple of decades [4–7]. Some articles have specifically reviewed the effect of types of feedstocks, types of reactors, and operating conditions, and some have reviewed models including reaction kinetics and the application of products and co-products. A general recommendation from these reviews emphasizes the need to investigate the coupled effect of textural, structural, and chemical char properties, which can affect the process conditions and reactivity. Other

than the operating conditions and biomass lignocellulosic composition, the inorganic or ash content of the biomass is a crucial parameter that may influence char reactivity. The mass of the inorganic constituents in feedstocks can range from less than 0.5% up to 15%, depending on the composition of the species [8,9]. The inorganic content is either present inherently in the raw biomass or externally added by impregnation with aqueous solutions. Significant research and development have been devoted to understanding the effect of mineral elements on char production and reactivity [8,10]. Most studies address the role of inorganic content, especially alkali and alkaline earth metals (AAEM), in char gasification to some extent, but only a few have investigated this in detail. The role of inorganic content incorporating a wide range of minerals in gasification is complex and not yet completely understood. A common observation has been the catalytic effect of AAEMs and the inhibiting effect of non-metallic minerals, which often varies with the type of reactor and the operating conditions. On the other hand, the operational issues related to the inorganic or ash content of biomass in gasifiers have been well reported [11,12]. Different pre-treatment (chemical, thermal, or mechanical) and post-treatment (gaseous and liquid products) approaches have been used to control and reduce the impact of inorganic species in thermochemical processes [13]. Biomass-derived chars are known to be relatively more reactive than coal chars. This is due to the char surface area, superior porosity, and the presence of inherent catalytic elements [14]. A detailed review on the gasification and combustion rates of biomass chars identified the inherent inorganic content, particularly soluble minerals, as being more influential than the char surface area and morphology [15].

The experimental and kinetics data obtained from the TGA and reactor level studies form the basis for the validation of the developed models, and thereby contribute to designing a pyrolysis reactor or gasifier and identifying the optimum operating conditions. Table A1 (Appendix A) shows primary and secondary reactions during pyrolysis and different reactions taking place in a typical biomass gasifier. For either process, understanding the reaction mechanism, kinetics, and the factors affecting the reactivity is important, and the role of inorganic content may be critical in gaining these insights. For example, the catalytic properties of inorganic metals during primary pyrolysis reactions are critical for the production of high-quality bio-oil and fine chemicals from biomass for meeting most of these targets. Similarly, the inorganic content affects the elimination of condensable organic compounds (tar) and methane during gasification [16]. Most studies have used the char produced from the pyrolysis of biomass as a starting feedstock for gasification. These studies inferred that the reactivity of char during gasification is governed by two major parameters: operating conditions (heating rate, pressure, temperature, and gasification agent concentration) [17,18] and char properties (porosity, chemical composition, and type of inorganic constituents) [19,20]. An appropriate understanding of the role of both inherent and impregnated inorganic content in char production and reactivity is essential for providing the best inputs to the reactor models. A recent article reviewed the catalytic effects of inherent minerals in biomass, especially AAEMs, on the pyrolysis process [21]. A few other articles also attempted to organize the growing body of knowledge on the fate of inorganics in pyrolysis and gasification [22–24]. However, a dedicated review of the role of the inorganic content of biomass in gasification reactivity is rare in the literature. More recently, an article reviewed the reaction mechanisms and kinetics models associated with the role of inorganic components in biomass char gasification [25]. Based on the literature survey, the identified knowledge gap is related to the lack of understanding of the impact of inherent and external inorganic contents on the reactivity of raw biomass and char during gasification in different reaction systems and under different conditions. The novelty of this review is to summarize and analyse the previous findings on the reactivity effects of inorganic content during biomass and char gasification to contribute towards more accurate modelling and design of the gasifiers.

2. Materials and Methods

A literature survey was conducted using keywords in the following direction: "biomass gasification" or "char gasification" → "biomass" → "ash" or "inorganic" or "AAEM" → "reactivity" or "catalytic", for the titles, abstracts, and keywords, using the Scopus platform. Figure 1 shows the distribution of the literature in the form of patents, research articles, and review articles. On the articles side, the returned results for a search within the time span 1977–2021 were: 6336 → 5812 → 1375 → 1011. These 1011 articles were then thoroughly scanned using various phrases related to the role or effect of inorganic contents on gasification performance, to return a result of about 106 articles. These included 9 review articles, out of which about 5 articles reviewed in part or in whole the catalytic or inhibitory effects of inorganic content during biomass gasification. On the patents side, the returned results for a search within the time span 1977–2021 were: 6341 → 3997 → 2410 → 1344. After thorough scanning of these 1344 patents as mentioned above, nearly 15 patents were found to explore the reactivity effects of the inorganic content of biomass. In the available literature on biomass inorganics, the ash-related operational challenges during gasification and the corresponding solutions were investigated and reviewed to a much greater extent than the reactivity effects. This underlines a challenge for investigating the reactivity of raw biomass and char, primarily because of the compositional complexity in the released volatiles, reactions within char, the variety of hypothesized modelling mechanisms, and a lack of experimental data [25,26].

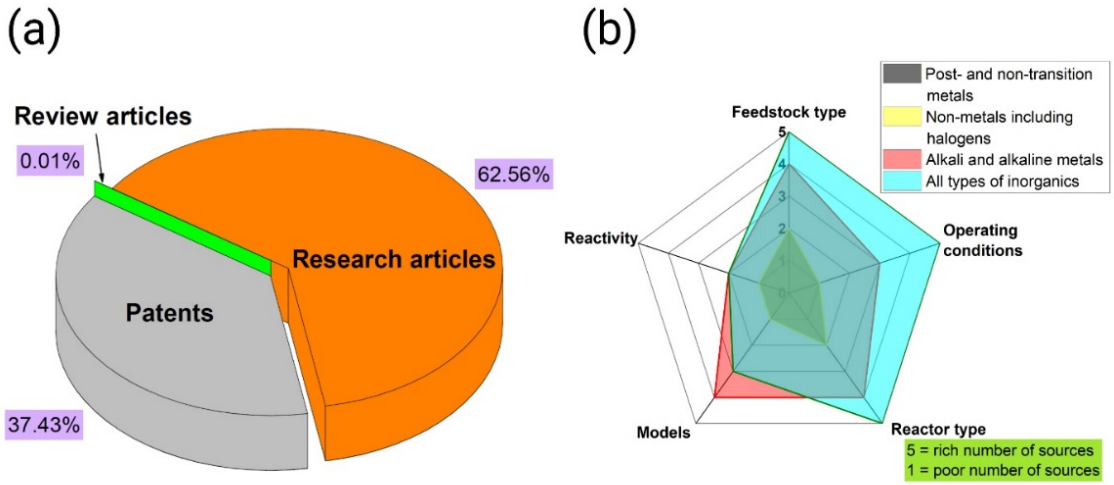

Figure 1. (**a**) Distribution of literature research sources in patents, reviews, and research articles; (**b**) the proposed review is expected to fill a knowledge gap on reactivity.

The objective of the present work is to provide a comprehensive review of the reactivity effects of the inorganic content of biomass on gasification reactions. The first section introduces the composition and characterization of inorganic content because it is important to understand the forms, occurrences, and classification of inorganic content before analysing its effects on gasification. The next section provides a brief overview of the effects of inorganic content in standalone pyrolysis studies because pyrolysis is known to be one of the important processes occurring in gasification. For gasification, different forms of feedstock were investigated in different set-ups to understand and investigate the effects of various inorganic species. For instance, some studies used raw biomass or washed biomass, some used char, and some used biomass or char impregnated or mixed with various inorganic species. Hence, the present study reviews the literature on the effects of inorganic content on biomass gasification by organizing the articles as follows:

(i) Effect of inherent inorganic content:

- Char gasification studies further classified into TGA and reactor studies;
- Biomass (raw/treated or washed) gasification studies.

(ii) Effect of externally added inorganic content:

- Char gasification studies (including tar reforming);
- Biomass (raw/treated) gasification studies.

These are the main experimental studies conducted over a range of biomass in either TGA or a reactor, mainly in the presence of CO_2 or steam as gasifying agents. The mechanisms for the catalytic effect of potassium and the inhibiting effect of silicon are also discussed. The subsequent section reviews the studies that attempted to incorporate the effect of the inorganic content in their kinetic models, along with the studies explaining the parameter of alkali index. Finally, the challenges and future research directions in the context of investigating the effects of inorganic content on biomass gasification are presented.

3. Results

3.1. Inorganic Content

Biomass contains different organic and inorganic elements depending on the biomass variety, environmental conditions, and harvesting time and approach. In a decreasing order, the common elements present in most biomasses are Ti, Mn, Na, P, Cl, Fe, Al, Si, K, Mg, Ca, N, H, O, and C [24]. However, there are many individual species for which the order of inorganic matter may be interchanged. The inorganic elements become a part of the both through both natural (plant growth and death) and anthropological (harvesting and processing operations) processes. Concerning the association of elements in feedstock, the literature on agricultural applications and biological conversion processes classifies inorganics into micro- and macronutrient groups. Cl, Cu, Mn, Ni, Mo, Zn, Fe, and B are micronutrients (concentrations $\leq$ 0.1%, dry basis), and Mg, P, S, K, Mg, and Ca are macronutrients (concentrations $\geq$ 0.1%, dry basis) [27]. Micronutrients modulate enzymatic functions, whereas macronutrients either play the role of osmotica or appear to be constituents of organic compounds [26]. Table 1 shows the existence of different inorganic elements in organic, inorganic, and dominant forms in lignocellulosic biomass. Oxalates, chlorides, sulphates, carbonates, nitrates, and amorphous structures in both forms (organic and inorganic) are the most mobile water-soluble phases. More details on the phases and chemical compositions of various minerals in biomass ash are available in the literature [24,28].

Table 1. Different forms of inorganic existence in lignocellulosic biomass [22,24].

Group	Organic Forms	Inorganic Forms	Dominant Forms
Alkali metals (K, Na)	Oxalate	Cation in liquid matter (Na^+, K^+), KNO_3, NaCl, KCl, $NaNO_3$	Often in ionic salt forms
Alkaline earth metals (Ca, Mg)	Carbonates, oxalates	Cation in liquid matter (Ca^{2+}, Mg^{2+}), $Ca_3(PO_4)_2$, $CaCl_2$, $Mg_3(PO_4)_2$, $MgCl_2$	Mg and Ca form structures with counterions of organic origin
Transition metals (Zn, Fe, Cd, Cu, Cr, Ni, Mn, Co)	Fe-chelates, Mn-carbohydrate	Cation in fluid matter (Mn^{2+}, Fe^{2+}, Cr^{3+}), metallic structures, iron oxide	Often in small (<2 µm) crystal structures which are introduced by harvesting and/or pre-/post-treatment
Post-transition metals (Pb, Al)	-	Aluminium hydroxide ($Al(OH)_3$), kaolinite	Highly variable and typically present in inorganic forms from different processing
Non-metals (S, P)	Covalently bound proteins, amino acids	Sulfite (SO_3^{2-}), sulfate anion (SO_4^{2-}), and phosphate anion (PO_4^{3-})	Differs with feedstock type

The mineral content and distribution of organic compounds, e.g., lignin, cellulose, hemicellulose, etc., show significant variations between different parts of the same tree or agricultural crop. For instance, pine needles, being richer in lipophilic extractives, especially in waxes, showed higher ash contents (2.2 wt.%, db) than the branches, bark, and cones, which had ash contents of 0.6 to 0.8 wt.%, db [29,30]. The thickness (age) of the bark also has an impact on the ash content; younger thin wood bark (2.3 wt.%, db) was found to contain significantly more inorganic matter than aged thick wood bark (0.6 wt.%, db) [31]. The ash content of feedstocks can also depend on structural (e.g., deviation in knots and grains) and environmental (e.g., atmospheric pressure, temperature, moisture) interactions during biomass growth [32]. Herbaceous species contain large quantities of K, S, and Cl compared to coal fly ash and wood [33]. These species commonly reveal higher ash contents than wood because grass can take up many more nutrients during growth due to rapid metabolism [23]. Among woods, hardwoods have a higher ash content than softwoods, as has been observed for pinewood and beechwood. Previous studies have also shown that wood ash content decreases with the age of the tree [34].

Inorganic materials in biomass and coal can be classified into various categories based on the nature of their occurrence. The inorganic matter in low-grade coal has been classified into discrete mineral structures, coordination complexes, and ion-exchangeable cations [35]. For biomass, inorganic matter can be separated into four categories: dissolved salts, organically bound material, included minerals, and excluded inorganic particles [28,36], as shown in Figure 2.

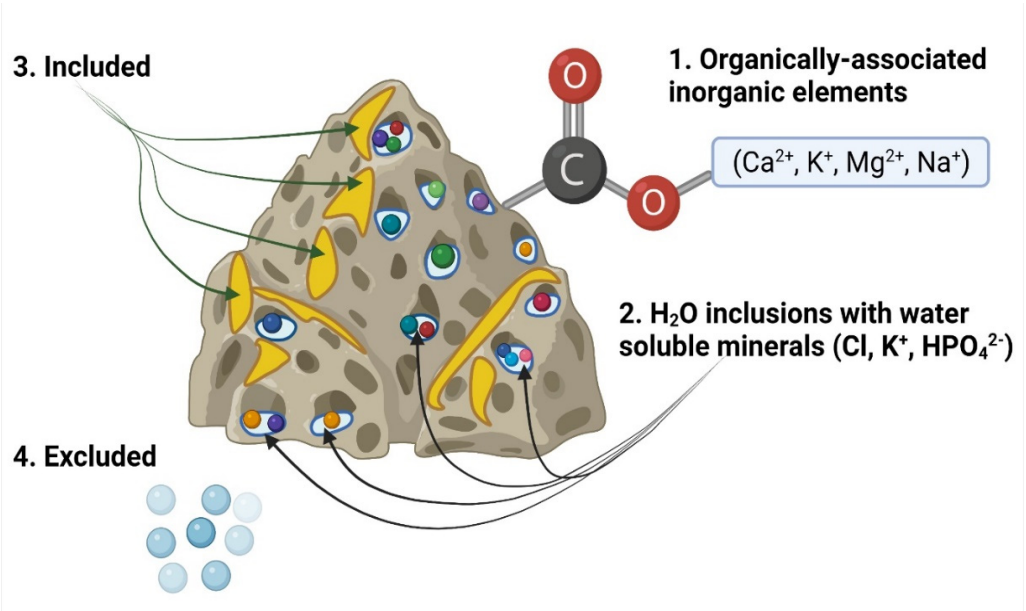

Figure 2. Inorganic constituents in biomass and their occurrence [28,36].

1. *Organically associated inorganic elements:* Inorganic species in the lignocellulosic matrix of biomass feedstocks include cations such as Na^+, K^+, Ca^{2+}, Mg^{2+}, Fe^{3+}, and Al^{3+} and non-metals such as organic Cl, S, and P attached with covalent bonds. Inorganic species in the organic phase are often associated with oxygen-containing functional groups such as carboxylic acids [26].
2. *Dissolved salts:* These originate from the liquid phases inside plants, and include cations dissolved in plant fluids, i.e., K^+, Na^+, and Ca^{2+}, and anions, i.e., SO_4^{2-}, Cl^-, and HPO_4^{2-}.
3. *Included minerals:* Discrete inorganic particles are located within the crystalline or non-crystalline lignocellulosic matrix. Typical minerals in wood are composed of Mg, Ca, and Si. The Ca element frequently appeared to be found in the form of calcium

oxalate CaC_2O_4, and Si exists as silicic acid $Si(OH)_4$, which provides strength to the plant tissue, often in herbaceous feedstock.

4. *Excluded minerals:* These include inorganics set free from the organic structure, such as clay minerals in the form of quartz, feldspars, or aluminosilicates, which are rich in K, Na, Ca, and Fe elements. Feedstocks can also contain impurities which originate from the various contaminants or soil.

This classification of inorganic content in biomass is discussed with experimental results on a sample biomass (olive stones) and hard coal (anthracite). Figure 3 shows an X-ray computed microtomography (*XμCT*) image of olive stones and anthracite. The signal intensity in the image is strongly interlinked with the mean atomic number of elements in feedstocks, similarly to the backscattered electron (BSE) image in scanning electron microscopy (SEM) [37]. Therefore, inorganic compounds with high atomic numbers can appear to be brighter during analysis than the organic structure of samples or other embedded structures which have lower atomic numbers. Olive stones, as shown in Figure 3a, represent an ash lean feedstock. The excluded mineral grains are visible due to the presence of contaminants such as soil, sand, or clay minerals that are mostly related to the transport and storage of olive stones in Tunisia and Spain. The amounts of the included species in olive stones are also less than in anthracite, as shown in Figure 3b. Most of the inorganic species in olive stones are found embedded within the organic, regular lignocellulosic matrix. Anthracite contains a fraction of the included inorganics that are less visible than the excluded inorganic matter, and the number of mineral inclusions varies widely among different coal particles. The included minerals in anthracite were found to contain Si, Ca, and Al compounds [37].

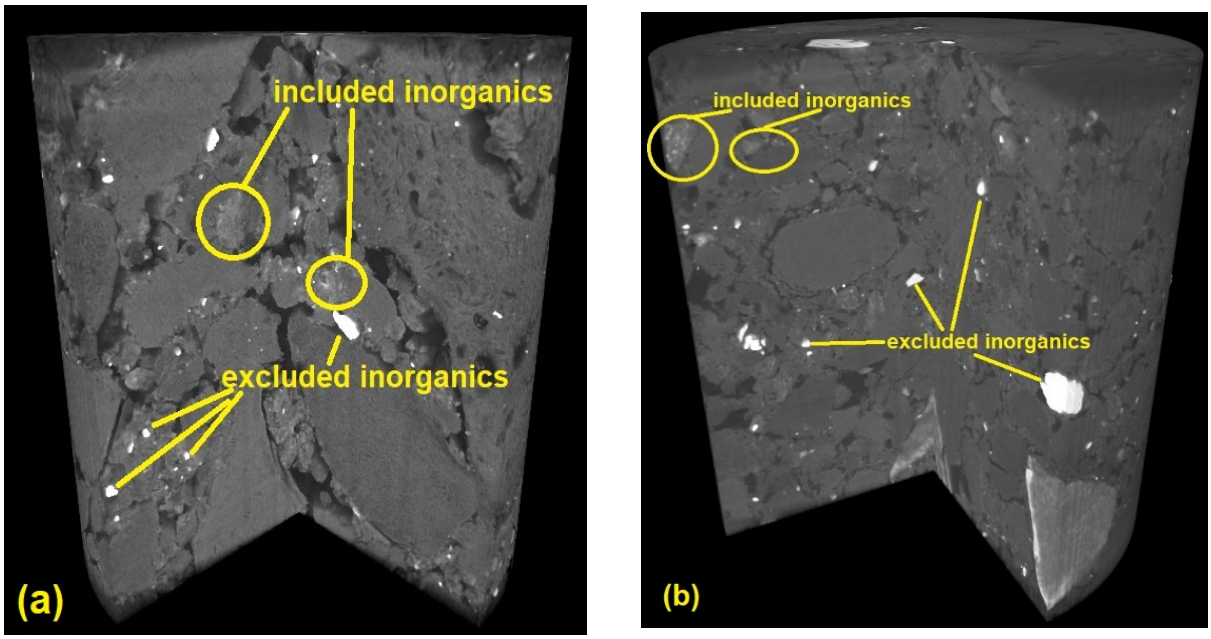

Figure 3. *XμCT* imaging analysis showing included and excluded inorganic matter for (**a**) olive stone and (**b**) anthracite [37].

3.2. Characterization of Inorganic Content

The analytical method has a strong influence on the proximate, ultimate, and ash composition of a solid fuel [38]. The most commonly used method for the inorganic content characterization of a solid fuel involves oxidation at high temperatures, followed by elemental analysis. During the fuel oxidation, inorganic elements are transformed into an oxide form, e.g., Na can be present as organically associated Na or a salt that can appear as Na_2O [26]. The information on the Na type of bonding is significant for the calculation of ash elemental composition. It was suggested to express the content of Na in the solid fuel

ash by using it either as an elemental base or as an oxide to avoid its underestimation in Na organically associated rich fuels, i.e., straw, low-rank coals, etc. Coal samples are typically oxidized at 815 °C, whereas biomass and waste are oxidized at 550 °C to avoid alkali vaporization [39]. The higher the oxidation temperature, the lower the content of the critical elements because of evaporation from the sample. Similarly, the selection of a chemical method for the ash analysis is also known to play an important role in the determination of element concentrations. The *X-ray fluorescence (XRF)* technique is a non-destructive method for elemental analysis which is fast and fully suitable for simultaneous quantitative determinations [40]. XRF analysis showed advantages over other spectrometric methods such as neutron activation analysis (NAA), which is expensive and not widely available. The mineral composition of biomass or char ash is often determined by *inductive coupled plasma—atomic emission spectroscopy/mass spectroscopy (ICP-AES/MS)* for the ash prepared with the ASTM D1102-84 method. ICP-AES requires procedures for the sample dissolution; that is, microwave digestion with a dangerous inorganic acid, such as hydrofluoric acid (HF), can deeply penetrate the tissue layer and destruct human bone [41]. The other equipment that can determine the mineral composition include *inductively coupled plasma—optical emission spectrometry (ICP-OES)*, which has more sensitive detection limits for most major and minor elements, i.e., Fe, K, Ca, etc., than XRF analysis [42,43]. The minerals are reported in terms of ppm or mg/kg or in weight percentages. Ash compositional analysis for various biomasses is reported in Table 2, which was carried out using the ICP-OES method. It is possible to classify biomass as low-ash (<2%), intermediate-ash (2–6%), or high-ash (>6%) biomass based on the ash content.

Another technique used in the semi-quantitative chemical analysis of inorganic matter is *SEM (scanning electron microscopy)* with secondary electrons (SE) and backscattered electrons (BSE) and combined with energy-dispersive X-ray (EDX) mapping [26]. Images based on SEs are known to visualize sample morphology and surface texture. BSE images indicate the signal intensity as a function of the sample atomic number in each specific location point. BSE-imaging is applied to differentiate sample phases by identifying mineral incorporations. Computer-controlled SEM (CCSEM) makes it possible to automatically evaluate the size, shape, quantity, and chemical composition of various mineral grains, e.g., in a feedstock or individual particles in a fly ash or soot sample. The SEM analysis is frequently combined with the *Fourier transform infrared spectroscopy (FTIR)*. The functional groups of raw feedstocks and biochar are recorded without special sample preparation. However, one of the limitations is related to the significant sample drying prior to FTIR analysis. *X-ray powder diffraction (XRD)* is most widely used for the identification of unknown crystalline materials, e.g., minerals and inorganic compounds [44]. XRD is known to perform well with single-phase mineral and homogenous inorganic materials. However, it does not demonstrate a high accuracy with heterogeneous inorganic layers [45]. *X-ray micro computerized tomography (XμCT)* is a non-destructive method for obtaining a digitalized, three-dimensional (3D) representation of organic and inorganic matter in both homogeneous and heterogeneous samples. The *XμCT* image analysis starts with image acquisition, which involves sample preparation, imaging, and reconstruction and has a strong impact on the analysis quality [46]. The properties commonly analysed by *XμCT* are related to the structural properties of the material, which are often parametrized into numerical values, e.g., porosity, thickness, tortuosity, autocorrelation, etc. [47]. The properties commonly analysed from pore/particle samples are surface area, volume, orientation, connectivity number, shape (circular or rectangular), etc. [48]. The organic and inorganic phases can be visually separated using the *XμCT* segmentation method that addresses thresholding and unsupervised classification. The dual energy *μCT* scanning instrument that uses a low voltage and samples of a small size is known to increase the quality of segmentation. However, *XμCT* scanning is recommended in combination with additional measurements using SEM-EDS or/and XRF techniques [49]. *XμCT* image analysis is limited to the qualitative analysis of inorganic matter. Further research and development are required to combine *XμCT* image analysis with EDX mapping to quantify inorganic compounds.

Table 2. Proximate, ultimate, and ash compositional analysis. HHV and LHV were calculated in MJ kg^{-1} as received.

Fuel	Pinewood							Beechwood [18]	Wheat Straw [18]	Alfalfa Straw [18]	Rice Husk [20]	Miscan-Thus [21]	Olive Stones [22]	Anthra-Cite [22]	Poultry Litter [23]
	Needles [13]	Bark [19]		Branches [19]	Cones [19]	Stumps [19]	Stem [18]								
		Small	Large												
Proximate and ultimate analysis (% on dry basis)															
Moisture	5.6	7.4	8	6.8	7.5	5.7	5.1	4.5	5.5	5.2	4.5	27.0	15.5	2.7	22.1
Ash	2.3	2.3	0.5	1	0.5	0.1	0.3	1.4	4.1	7.4	21.7	3.4	0.8	9.9	17.5
Volatiles	78.8	76.7	70.9	79.9	78.3	86.5	86.6	79.4	77.5	75.9	64.3	77.8	76	15.8	73.7
HHV	21.3	19.5	21.3	20.9	20	21.2	21.6	20.2	18.8	19.7	15.5	14.1	20.3	32.2	19.7
LHV	20	18.2	20.1	19.6	18.8	19.8	20.2	19	17.5	16.9	14.5	12.5	18.8	31.5	13.5
C	51.8	49.5	54.5	51.4	51.1	52.3	53.1	50.7	46.6	42.5	37.8	48.5	44.8	72.3	35.1
H	6.3	5.6	5.4	5.9	5.5	6	6.5	5.9	6.1	6.7	4.7	6.0	5.8	2.9	4.1
O	38.2	42	39.4	41.2	42.6	41.5	40	41.9	42.5	43.1	0.3	41.6	48.3	13.2	30.8
N	1.4	0.6	0.2	0.5	0.3	0.1	0.06	0.13	0.6	0.3	35.5	0.5	0.2	1.0	4.2
S	0.1	0.04	0.02	0.03	0.02	<0.01	<0.01	0.02	0.1	0.03	0.03	0.07	0.1	0.7	0.6
Ash compositional analysis (mg kg^{-1} on dry basis)															
Cl	0.02	0.01	<0.01	<0.01	0.01	0.01	0.01	0.02	0.1	0.5	0.05	0.3	0.01	0.03	0.5
Al	250	550	250	150	150	40	10	10	150	600	70	270	100	12,000	5500
Ca	2450	4700	1200	1300	250	500	600	2000	2500	12,900	750	1100	1650	3500	7800
Fe	70	60	60	60	20	30	20	10	200	-	80	270	70	7200	400
K	5600	35	800	2000	2000	200	200	3600	11,000	28,000	2500	7900	1600	2000	1600
Mg	750	90	200	400	350	100	100	600	750	1400	400	540	150	350	2000
Na	25	10	10	<10	210	<10	30	100	150	1000	70	340	300	2000	2000
P	1500	75	150	400	350	<10	6	150	550	1900	600	740	100	800	6800
Si	400	15	350	400	350	150	50	200	8500	2000	9850	6200	1800	41,000	9200
Ti	4	1	2	6	7	1	2	8	10	3	5	13	10	700	40

3.3. Overview of the Effects of Inorganic Content in Pyrolysis

Pyrolysis is a complex thermochemical process which cracks biomass into tar/bio-oil (liquid fraction), char (solid fraction), and non-condensable gases in different proportions depending on the biomass composition, operating conditions, reaction pathways, reactor design, etc. [50–52]. Though the process is primarily focussed on bio-oil production, the interest and research on employing different types of pyrolysis have been growing for charcoal and coke formation [53]. An extensive literature is available on different types of pyrolysis processes, as reported in Table A2 (Appendix B) with respect to chemistry, kinetics, reactors, and other practical aspects [34,52,54]. Bio-oil and biochar obtained from the pyrolysis process have attracted much interest because of their potential applications in diverse sectors. The heterogeneity of biomass in terms of composition and characteristics poses a challenge for producing a fuel or a material with the desired properties. It can also be seen an opportunity to produce materials with various properties in such applications as metal ore reduction or soil sequestration. Different factors such as pyrolysis conditions, reactor design, the organic and inorganic content of biomass, and the catalyst affect the yield and properties of the products to different extents. Many experimental and modelling studies have attempted to address the impact of these factors by using a single lignocellulosic component or a mix of them, as well as raw or pre-treated biomass [26]. Among these, the most challenging is the effect of biomass inorganic content interactions, which creates a large scope for further investigation. A review of some of the experimental studies investigating the effects of inorganic content on the pyrolysis of various biomasses in reactors and/or TGA is given in Table A3 (Appendix C) first for inherent species and second for externally added species.

Most of the studies focussed on AAEMs for their relatively higher effect on pyrolysis behaviour, while few addressed the effects of trace metals and potentially toxic elements (PTEs) [55]. The primary factors associated with the effect are the onset temperature of thermal decomposition, the reaction pathways and rates, and the product distributions, composition, and properties. The temperature and heating rate at which chars are prepared influences the chemical form of the metal, with different forms showing different effects on product quality. For instance, during the pyrolysis of cellulose above 650 °C, potassium is known to change its state from being predominantly in the K_2CO_3/KOH/K_2O form to being dispersed as a metal throughout the char matrix prepared from potassium-acetate-doped cellulose [29]. The inorganic elements have been found to affect the decomposition of the biomass organic matrix at a molecular level. The composition and distribution of alkali metals left in the char matrix and the release of alkali metals also affect the reactivity of chars. One of the studies compared the effect of ash with that of lignin and found a dominant ash effect on pyrolysis yields, though lignin governed the higher-molecular-weight compounds in bio-oil [9].

TGA studies found that potassium affects the biomass decomposition temperature and formation of char, whereas magnesium and calcium influence the decomposition rate. A simple approach for understanding the role of specific inorganic constituents is to demineralize the raw biomass and add a known quantity of a metallic species of interest. To understand the reactivity or catalytic effect of a particular constituent, the externally added constituent is usually similar to the actual concentration in raw biomass. A notable catalytic effect of potassium on the inhibition of levoglucosan formation was confirmed using analytical Py-GC/MS [56]. K and Mg significantly affected the yields of pyrolysis in comparison to Ca. For biomass impregnated with inorganic species, the raw biomass is often pre-treated using water or acid wash to remove the minerals. The removal of minerals not only increases the bio-oil yield but also provides benefits such as the protection of catalyst and combustor [57]. In the case of wash with strong inorganic acids, some of the amorphous cellulosic components may also become dissolved, affecting the organic composition of biomass. In their study on the pyrolysis of various woody and herbaceous biomasses, the demineralization increased the yield of volatiles, the rate of decomposition, and the initial decomposition temperature for high-ash biomass such as

rice husk, groundnut shell, and coir pith [58]. The effect was further increased for these biomasses when they were impregnated with potassium and zinc. The authors attributed the behaviour to the contents of lignin, potassium, and zinc in the biomass and developed the following correlation:

$$\Delta V = -0.964\left(L^{1.095} X_K^{1.3727} X_Z^{0.0996}\right) + 7.192 \quad (1)$$

where ΔV is the change in the percentage yield of volatiles due to mineralization, L = is the lignin content (wt.%) of the biomass, X_K is the fraction of potassium in silica-free ash, and X_Z is the fraction of zinc in silica-free ash. Among the AAEMs, potassium is the most widely studied metal for its catalytic effect on biomass pyrolysis, with various attempts having been made to incorporate that effect in the proposed kinetic models for the process [59,60]. More details on the effect of the inorganic content of biomass on the yields and properties of the gas, liquid, and solid products of pyrolysis are available in the literature [21].

In an autothermal gasification reactor, the heat required for the processes of drying, pyrolysis, and reduction is provided through the oxidation or combustion process. From the kinetics perspective, pyrolysis and oxidation are faster than the gasification step. Pyrolysis is governed by both chemical reactions and heat transfer, while gasification is primarily governed by chemical reactions [60]. This emphasizes the need to better understand the gasification kinetics not only to design the reactor but also to control the char going to the oxidation zone for providing the required heat. Inorganic content being one of the important factors influencing the reactivity, we now discuss its effects on biomass gasification first based on differently classified experimental studies, and then based on modelling studies.

3.4. Effect of Inherent Inorganic Content on Char Gasification

Among various approaches, the highest number of studies investigated char gasification in the presence of agents such as CO_2 and H_2O, predominantly in a TGA set-up, to understand the role of inorganic content. Some studies used a mixture of gas species for char gasification to analyse the reaction conditions in a real gasifier. In a mixed atmosphere of CO_2 and H_2O, Guizani et al. noted that the reactivity of these two gasifying agents can be additive, competitive, or even synergistic [61]. The synergistic interaction between CO_2 and H_2O during char gasification may be explained by the development of mesopores by H_2O, allowing for a more rapid entry of CO_2 into the micropores [62]. As shown in Figure 4, the increasing concentration of minerals with the conversion indicates a higher retention in the char, while those with constant or decreasing concentrations indicate that the species is instead being volatilized.

The H_2O gasification atmosphere not only retains higher Mg, K, and Ca in char compared to the CO_2 atmosphere, but also a high amount of Si was observed which is known to inhibit the reaction [61]. In addition, Si is known to volatilize in a CO_2 atmosphere, while it remains in the char matrix during H_2O gasification. A higher internal char porosity has been reported in H_2O activation than in CO_2 activation at the equivalent conversion levels due to the small size of the molecules and an improved diffusivity, leading to a more volumetric gasification reaction. H_2O gasification supports the development of 1 nm micropores along with mesopores, whereas CO_2 gasification mainly develops micropores in the range of 10–20 Å. CO_2 gasification suggests a limited diffusion of CO_2 molecules inside the char particle and an accentuated surface reaction leading to a sponge-like surface at high conversion rates and, thus, to a gasification reaction progressing over almost all the surface in an equivalent way and culminating in Si release [61]. Except for biomasses with higher Si contents, most biomass has shown a direct relation between inorganic contents and the gasification reaction rate [63–65].

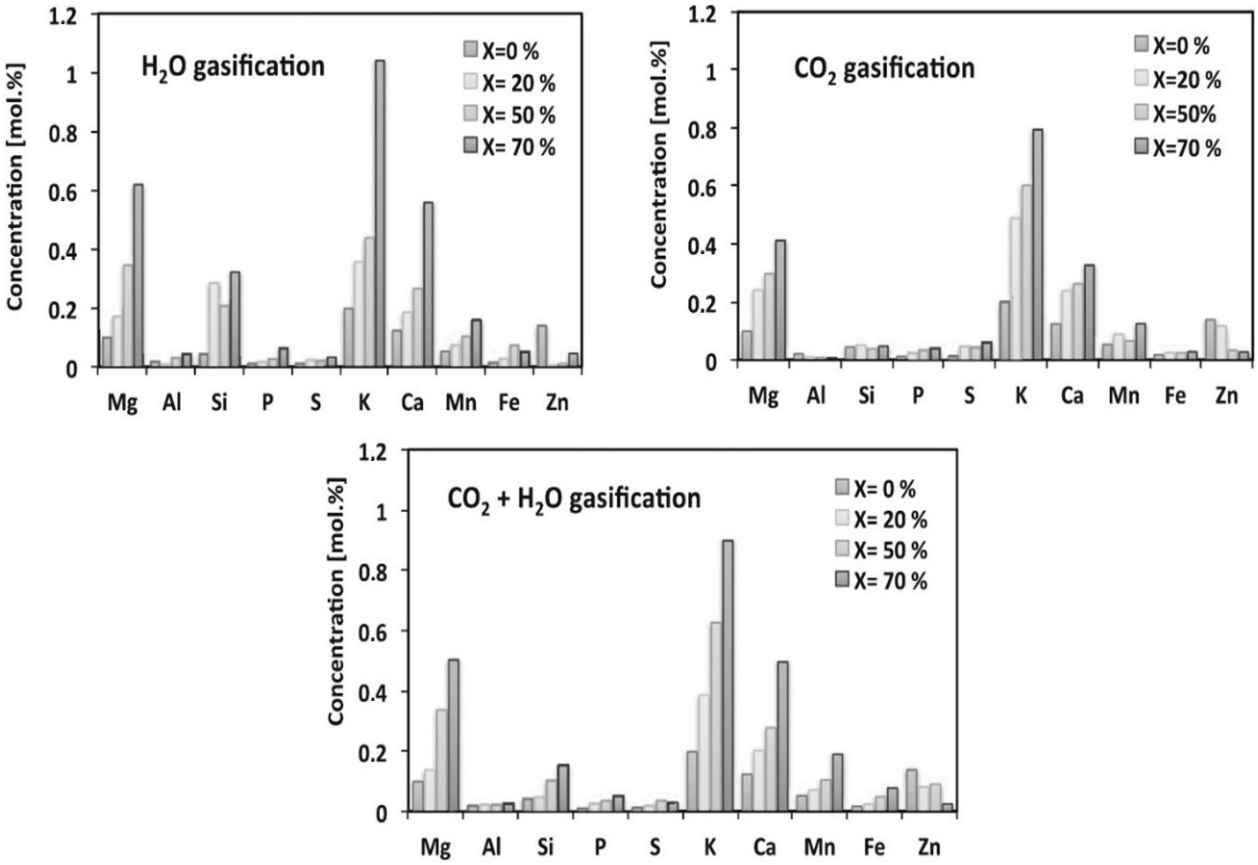

Figure 4. Concentration of inorganic components in the beechwood char (mol.%) along the gasification with steam, CO_2, and combined H_2O and CO_2 agents at 900 °C [61].

Table 3 shows the experimental studies that investigated the effect of inherent inorganic content on char gasification conducted in TGA under CO_2 and H_2O atmospheres. For CO_2 gasification, the apparent activation energy values are relatively higher (200–250 kJ/mol) than for H_2O gasification (130–170 kJ/mol) [66]. In one of their extensive experimental and kinetic modelling studies on 21 different biomass chars, Dupont et al. confirmed that the average gasification reaction rate differed by a factor of 3.5 even though all the samples were prepared and treated under the same conditions [67]. The variations in reactivity were mainly owing to the inorganic elements, where potassium offered the highest catalytic effect and silica imposed an inhibitory effect on char gasification. Similar observations have been confirmed by several other studies on different biomasses, which specifically reported the catalytic effect of potassium inherent in biomass [68–70]. The net effect of various inorganic species is dependent on the amount of a particular component in the ash. Herbaceous feedstocks such as straw and miscanthus with higher K and Na than wood showed lower reactivity because of much higher Si contents [71]. For feedstocks such as algae with higher amounts of phosphorus (P), the inhibitory effect is integrated with that of Si [72]. Unlike the unidirectional influences of K and Si, the role of Ca is not clear, as Ca has been reported in different studies as playing a catalytic as well as a hindering role in char gasification. Steam gasification using a fluidized-bed reactor was reported in numerous studies. The observable increase in the catalytic activity in the fluidized-bed gasification reactor was associated with Ca-enrichment on the surface [73,74]. Kramb et al. reported similar findings for CO_2 gasification [75]. Char transformation was related to Ca-doping in the biomass fuel and the resulting interaction of the ash with the bed material.

Raw biomass contains AAEMs in the form of the aqueous phase, salts, as well as carboxyl and other organic functional groups [76,77]. When the biomass undergoes pyrolysis, inherent AAEMs partly vaporize with lignocellulosic decomposition, but most

remain in the char. During gasification, as the conversion proceeds, most of the AAEMs are released from the char, and the influence of inorganic species becomes dominant over other factors such as surface area. The impact of AAEM release from the feedstock matrix has been observed in the transformation of the char structure and morphology. The natural porosity can be maintained in chars during low-heating-rate pyrolysis, whereas chars from high-heating-rate pyrolysis form larger cavities [34]. The larger surface area of chars formed at high heating rates with greater oxygen and hydrogen contents in a char matrix led to more available active sites for the gasification reaction, leading to a stronger catalytic effect of AAEMs.

Previous investigations have shown that the gasification reactivity of both wood and herbaceous biomass decreases at temperatures above 1000 °C and in H_2O or CO_2 environments [77,78]. The vaporization of K and Si from the feedstock can lead to the deactivation of solid char during gasification tests [73]. For high-ash biomass such as rice husks (>10 wt.%), the inorganic composition affects the kinetics of steam gasification more than the physicochemical properties of the carbon matrix [25]. At temperatures $\geq$ 900 °C, the release of ~12–16% of Ca/Mg and ~12–34% of K/Na takes place during steam gasification [79]. Figure 5 shows an illustration of the structural and inorganic transformations in biomass during char formation and gasification. At temperatures $\geq$ 700 °C, the release of KCl and KOH from the char is significant, with KOH likely originating from the decomposition of K or K_2CO_3 in the char structure. For Si-rich biomass above 700 °C, K and Ca become partially incorporated into the Si-rich outer surface, but this is limited by the presence of organic material. Since most of the studies investigated the effect of inorganic components, in particular K and Si, some of the studies proposed the mechanism to explain their effect on gasification performance [17,76,80].

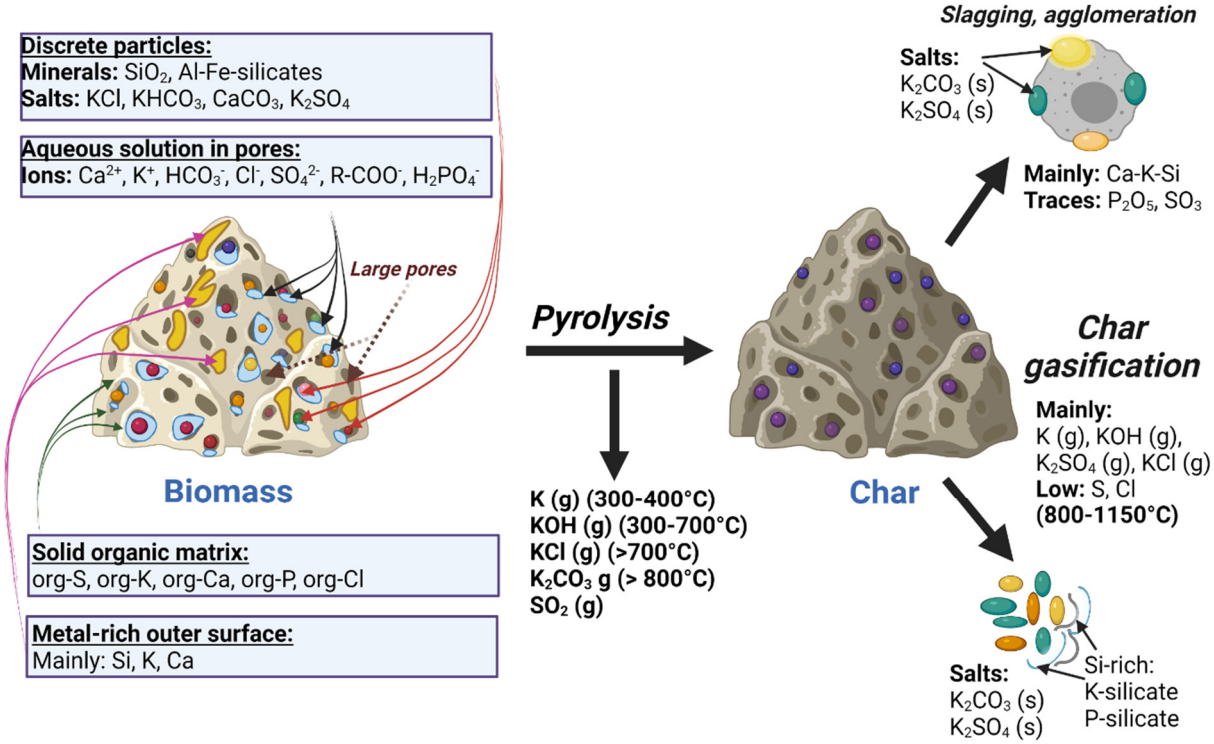

Figure 5. Inorganic transformation mechanisms and structural changes in feedstock during char formation and gasification [14,76,80].

Table 3. Experimental studies investigating the effects of inherent inorganic content on the gasification of char.

Ref.	Gasification System and Feedstock	Char Production	Main Findings
		Gasification in TGA	
[66]	TGA at 725, 750, and 800 °C; CO_2: 60 mL/min; p_{H2O}: 1.7, 3.2, 19.9, and 47.4 kPa in N_2. Grapefruit skin	Fixed-bed quartz tube reactor at 700 °C for 2 h in N_2 at 150 mL/min	E_a values for CO_2 gasification: 200–250 kJ/mol; for steam gasification: 130–170 kJ/mol. K mostly contributed to the increased reactivity compared to Ca, Na, and Si. Decreasing the inorganic content of the char through washing reduced CO_2 reactivity.
[81]	Macro TGA, 900 °C/min till 927 °C; 20% H_2O in N_2 (4 L/min) Beechwood	Refractory steel box swept with N_2 in muffle furnace, at 2.6 and 12 °C/min, kept for 8 min at 900 °C	The ash content (mainly the elements Ca and K) in beechwood char was proportional to its initial apparent reactivity of gasification. Individual component effects could not be distinguished in the study.
[82]	TGA, 10 °C/ min till 600–1000 °C; 50% CO_2 with argon. Pinewood, birchwood	Fixed-bed reactor at 500 °C for 150 min	The inorganic content of the chars was low, around 1%, and the decomposition kinetics for both chars revealed considerable similarities in CO_2 environments. The activation energy (E_a) for the gasification step was 262–263 kJ/mol.
[60]	TGA, 24 °C/min to 750–900 °C, 1 atm using p_{H2O} in N_2 = 0 to 0.27 MPa. Woody biomass	TGA, <10 °C/min to 450 °C, held for 4 h in N_2 flow of 0.05 L/min	The concentration of inorganic elements increased with the conversion, which increased their catalytic or inhibitor effect. K showed catalytic and Si showed inhibiting effects on the steam gasification of char.
[71]	TGA (800–1300 °C) and aerosol-based method (1100–1300 °C) using CO_2 and H_2O. Wood, straw, miscanthus	Tubular fixed-bed reactor at 600–800 °C in N_2 (5 KW)	Straw and miscanthus chars had higher contents of alkali metals (K, Na), but showed lower reactivities than wood due to the high Si content in herbaceous feedstock and the formation of an inorganic layer on the outer surface. This can lead to a blockage that further hinders gas diffusion to the carbonaceous surface.
[72]	TGA, 800 °C, using a mixture of H_2O/N_2 (p_{H2O} = 0.2 bar) flow of 0.05 L/min. Algal and lignocellulosic biomass	TGA, 24 °C/min to 450°C in N_2 flow of 0.05 L/min for 1 h and then to 800 °C	Phosphorus (P) was included in the expression because of its higher percentage in algae. For feedstocks with K/(Si + P) > 1, the reaction rate remained constant during mostly the entire reaction and then it slightly increased at higher conversions. For feedstocks with K/(Si + P) < 1, the reaction rate decreased during the reaction.
[83]	TGA, CO_2 flow of 200 mL/min isothermally at 900 °C for 40 min. Corn stalk, metasequoia pruning	TGA/DSC, 200 mL/min N_2, 50 °C/min up to 900 °C, and maintained for 10 min	Torrefaction concentrated AAEMs in char, leading to higher CO_2 gasification reactivity than the raw biomass. Torrefied chars were richer in active Ca, K, and Na than the original feedstocks. Char gasification, as the rate-determining step, can be improved by torrefaction.
[84]	TGA and Setaram TAG24 analyser, 1 atm, 700–1000 °C, using 75/25 vol.% N_2/H_2O. 12 biomass (hardwoods, softwoods)	Bubbling fluidized-bed reactor, 1000 °C in N_2 flow of 1.365 L/min	K, Na, and Mg showed a positive effect, while Si, P, and Ca showed a negative effect on char reactivity. The activation energy for gasification ranged between 59 and 196 kJ/mol.
[85]	TGA isothermal process 700–800 °C for raw char and washed char, 7.6 mol% H_2O in N_2. Pine wood	Obtained from scrubber sediment tank of entrained-flow gasifier, 900–1150 °C, air; TGA at 950 °C in N_2 for 3 h	For conversions < 70%, the char surface area is a predominant factor irrespective of the inorganic content. At conversions > 70%, the catalytic effect of K becomes predominant.

Table 3. *Cont.*

Ref.	Gasification System and Feedstock	Char Production	Main Findings
		Gasification in TGA	
[86]	Macro-TGA 800 °C, 20 vol% H_2O in N_2 flow of 5 L/min. Rice husks, sunflower seed shells	Holder with 30–50 g sample in furnace heated at 10 °C/min to 450 °C, held for 1 h, in N_2 flow of 1 L/min	For two biomasses, the inorganic composition affected gasification kinetics more than the physicochemical properties of the carbon matrix. Inorganics also affected the microporosity and the number of surface functions.
		Gasification in reactor	
[79]	Reactor diameter of 30 mm and a length of 500 mm (drop tube furnace) using CO_2 or H_2O and N_2 at 900–1000 °C. Woody biomass, lawn grass	Obtained from pilot-scale entrained-flow gasifier (5 kW) using steam and oxygen	For H_2O gasification, (K_2O + Na_2O) showed a stronger effect than it did for CO_2 gasification. The CO_2 gasification rates of different chars linearly depended on the concentrations of the predominant inorganic compounds (K and Ca).
[77]	Quartz fixed-bed reactor 8.2% vol. H_2O in 3 L/min of argon, 750 °C. Mallee leaf, wood, bark	Quartz fixed-bed reactor at 10 °C/min to 750 °C, held for 15 min; char was later acid-treated	Acid treatment reduced AAEM content and the catalytic effect on gasification reactivity, which also depended on the char carbon structure and catalyst dispersion. AAEMs had an insignificant effect on the water–gas shift reaction.
[69]	15 mm diameter quartz tube reactor; 27.3 °C/min at 850 °C, H_2O-N_2 or H_2O-H_2-N_2 mixture at 0.2 L/min. Japanese bamboo, cedar	Horizontal screw-conveyor reactor 47 s, 500 °C, 5 to 5.5 °C/s and 1 atm	Acid washing of chars removed K and Na without changing Mg and Ca, and lowered the gasification reactivities, confirming the catalytic effect of K.
[87]	Lab-scale semi-batch reactor in H_2O at 750–900 °C (0.2 bar). Food waste (dog food)	Lab-scale semi-batch reactor in argon at 900 °C for 1 h	As the conversion increased from 0.1 to 0.9, the reactivity increased mainly due to an increase in the pre-exponential factor, indicating an increased adsorption rate of the gasifying agent to the char surface.
[88]	Quartz fixed-bed reactor, fed at 900 °C, H_2O, flow rate 200 mL/min, 2–25 min. Maize stalk, rice husk, cotton stalk	Quartz fixed-bed reactor, fed at 900 °C, N_2, 10–300 s	Char gasification led to a further loss of 12–34% of the alkali metals. The Na concentration remained constant, but the H_2O reactivity changed along with the dropping concentrations of Mg, Ca, and K.
[78]	Quartz fixed-bed reactor at 785 to 865 °C in 100% CO_2 flow of 750 mL/min. Pinewood sawdust pellets and coal	Fixed-bed reactor at 6 °C/min to 900 °C, held for 3 h in N_2 flow of 1.5 L/min	During co-pyrolysis, calcium in the biomass reacted with aluminosilicate in the coal to form catalytically inactive $Ca_2Al_2SiO_7$ crystals, which lowered gasification reactivity.

3.5. Mechanisms for Potassium, Calcium, and Silica Effects

The alkali carbonates are generally known to enhance the rate of steam and carbon dioxide gasification through an oxidation–reduction catalytic effect on the process with the formation of different intermediates. For both CO_2 and H_2O gasification, the most commonly used mechanism for K transformation is the one proposed by McKee [89]:

$$\text{Carbothermic reduction: } K_2CO_{3(s)} + 2C_{(s)} \leftrightarrow 2K_{(g)} + 3CO_{(g)}$$

$$\text{Oxidation: } 2K_{(g)} + CO_{2(g)} \leftrightarrow K_2O + CO_{(g)}$$

$$\text{Carbonate formation: } K_2O + CO_{2(g)} \leftrightarrow K_2CO_{3(s)}$$

This mechanism was further modified by Moulijn et al. as follows, but it is not confirmed whether the second and third steps are independent or integrated; the same applies

for the rate-determining steps [90]. The decomposition of the surface complexes (CO) is accelerated by the destabilization of these complexes. It is believed that the mechanism is also applicable to the H_2O and O_2 media of gasification.

$$CO_2 + K_xO_y \leftrightarrow CO + K_xO_{y+1}$$

$$K_xO_{y+1} + C \rightarrow K_xO_y + (CO)$$

$$(CO) \leftrightarrow CO$$

A general mechanism used to characterize steam gasification is summarized as shown in Figure 6 along with the following chemical reactions, where M denotes an alkali metal [91]:

$$M_2CO_{3(s)} + 2C_{(s)} \leftrightarrow 2M_{(g)} + 3CO_{(g)}$$

$$2M_{(g)} + 2H_2O_{(g)} \leftrightarrow 2MOH_{(s,\,l)} + H_{2(g)}$$

$$2MOH_{(s,\,l)} + CO_{(g)} \leftrightarrow M_2CO_{3(s,l)} + H_{2(g)}$$

The first reaction in this mechanism is inhibited by increasing amounts of CO, and hence it is likely to be a rate-determining step. Figure 6 shows that the biomass solid char that contains K–O–C groups inside the carbonaceous matrix is expected to be less reactive due to the reactions on the solid–gas interface. The K-O-C phenolate groups break and form again, contributing to the condensation of aromatic rings and concurrently leading to the formation of larger aromatic rings [92]. The steam gasification rate of the carbon-supporting alkali metal salts was found to be proportional to the amount of trapped oxygen in the form of an M-O-C bond on the carbon surface [92,93]. The rate of CO_2 formation was almost proportional to the gasification rate, while that of CO was very small and almost constant irrespective of the salt supported [93].

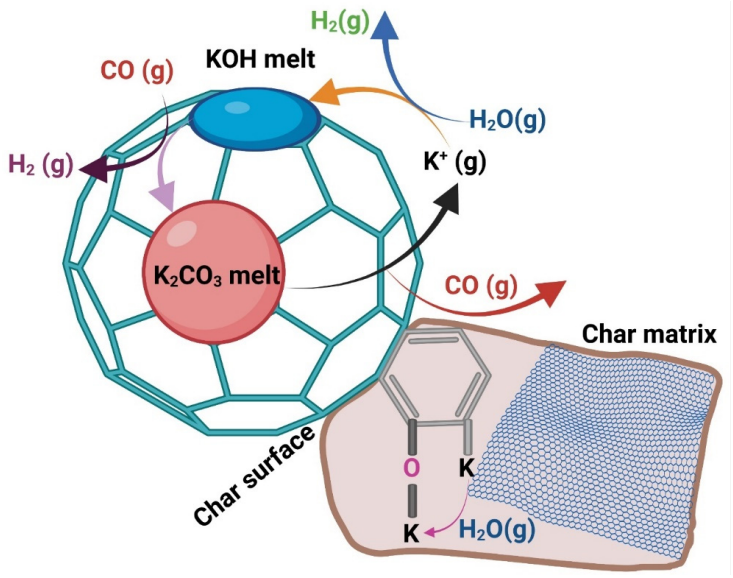

Figure 6. Mechanism of the interaction of potassium compounds with the carbonaceous char matrix during steam gasification [91,94].

Silica or Si-containing species were found by most of the studies examined to have a negative or an inhibiting effect on the gasification reaction rates. Strandberg et al. reported the melting of a char shell as a reason for the decrease in conversion rate at a higher conversion degree during high-temperature gasification [95]. Figure 7 confirms the encapsulating effect of molten Si-containing inorganics, forming an ash layer that acts as a diffusion barrier preventing carbon oxidation from taking place in the kinetically controlled regime, especially at higher conversions. This effect was predominant for wheat

straw char but significantly lower for pine wood char because of its low Si and high Ca and Mg contents [96]. Another study on the reactivities of pinewood and rice husk chars investigated in oxidative and CO_2 environments also confirmed the formation of glassy char shells [97]. The amorphous silicates dispersed in the carbonaceous char matrix can cause heterogeneous softening in Si-rich rice husks during high-temperature treatment due to the molecular disordered char structure. The shapes of the chars in each of these studies remained preserved in the temperature range of 800–1600 °C. However, the reactivities of both chars from rice husk and pinewood were similar. This indicated that the effect of silicon oxides on char reactivity was lower than the alkali metals. Though K and Si are known to have independent effects on char reactivity, some studies have reported the interaction of these two components as causing slag formation and, thus, as decreasing the reactivity of char during gasifier operation [96].

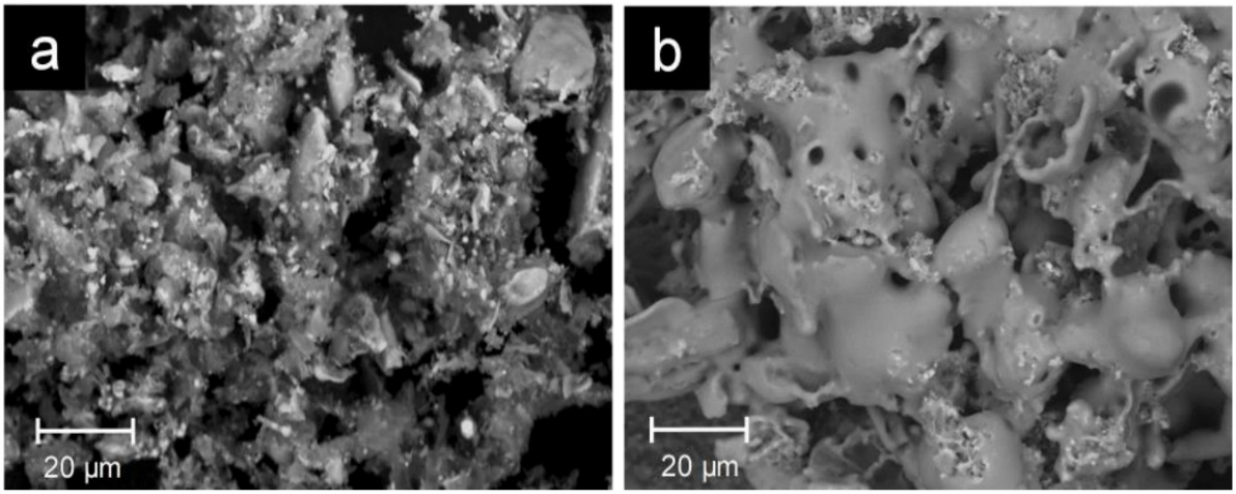

Figure 7. SEM of residues from interrupted isothermal TGA gasification of wheat straw char at 850 °C at (**a**) 25% conversion and (**b**) 90% conversion [96].

During the biomass gasification process, inorganic components such as Si and Al have been reported as reacting with AAEMs such as Ca and K to form aluminosilicates and silicates [68,98,99]. With the increased conversion, the migration of AAEMs becomes significantly influenced by other components such as Si, Al, and P. Alkaline earth metals are known to have a greater ionic potential than alkali metals, which makes them more prone to react with silica [100]. A mechanism when K is present only on the surface without incorporation into the carbonaceous char matrix suggests that mostly weaker bonds were formed. Thus, a higher reactivity can be expected than in carbonaceous matrix of char containing C-O-K phenolate groups. However, this can strongly depend on the type of K-containing compounds. Since the AAEMs impregnation procedure is not standardized, it is not easy to identify a conclusive trend in the composition of K-containing compounds due to the strong dependence on the organic and inorganic composition of feedstocks and their blends and the broad range of operating conditions used in gasification. More research is required on the type of compounds remaining on the char surface and intercalating into the carbonaceous matrix. The water-soluble salts determine the catalytic gasification rate when C-O-K groups on the carbonaceous matrix surface are not formed [101]. In case the K_2CO_3 has good contact with the char matrix, an increase in CO_2 reactivity can be expected with the increasing content of K until its saturation. This emphasizes the importance of the operating temperature on the transformation of inorganics causing the differences in morphology. Both mechanisms for K and Si transformation during gasification cause the impact on the inner part of the char and on the surface. Thus, a comprehensive overview of inorganics' reactivity can be provided when individual pathways for each element are combined.

In fluidized-bed gasification systems, the reactivity of K is related to the interaction between ash and the bed material. K, added as K_2CO_3, was enriched on the surface of the bed material during ash layer formation [102]. The catalytic activity during char gasification was attributed to the transfer of K from the ash layer to the char matrix. As the experiments were performed under steam gasification conditions, the transfer of K to the char was presumably as gaseous KOH. Similar observations were reported by Larsson et al., where K was added to the industrial-scale gasification plant GoBiGas, when the ash composition of the input biomass stream was alkali-lean [103]. The aim was to achieve a balance of catalytically active compounds in the reactor. In fluidized-bed gasification systems, the bed material acts as a carrier material for K and as such as an enabler. However, the actual reactivity is based on the transfer of K from the gas phase to the char matrix [102].

By contrast, the catalytic activity achieved by Ca is associated with solid–solid reactions. In fluidized-bed gasification, Ca, analogous to K, is enriched on the surface of the bed material during ash layer formation. From the available published information, a conclusive mechanism cannot yet be derived for the catalytic activity involving Ca. Nevertheless, a rough basis for the formulation of a comprehensive mechanism can already be outlined. Experiments using the adsorption of CO as an indicator for the identification of active sites on the particle surface showed the existence of CaO on particle surface after the interaction with biomass ash. Thus, it can be stated that during ash layer formation CaO is formed [103]. It was observed that the enrichment of CaO on the particle surface positively influenced the reaction kinetics of typical gasification reactions [104]. A rate expression using ash-layered bed material was derived to represent the increased catalytic activity of the bed material after CaO enrichment in the ash layer [105]. The positive effect of CaO on the reactivity of char transformation and tar reforming in gasification has been reported on multiple occasions [106,107]. In summary, it can be stated that the effect of Ca with regards of the catalytic activity is less strong in comparison to K, as the effect is derived from Ca being present in its solid state. The positive effects resulting from the inorganic components of biomass were summarized [107].

3.6. Pre-Treatment of Feedstocks

Since inorganics have been correlated with gasification kinetics, it is important to understand how the mineral composition of feedstocks can be tuned using chemical and mechanical pre-treatment methods. The inherent inorganics have a significant impact on the kinetics in gasification, whereas K tends to have the highest catalytic activity, concurrently increasing the gasification reactivity. The pre-treatment methods which are known to impact the reactivity of non-treated feedstocks or chars in gasification through the removal or addition of minerals are classified according to the selection of chemical, thermochemical, and mechanical processes, as shown in Figure 8.

Demineralization is a key chemical pre-treatment step for influencing the gasification reactivity of biomass, whereas the concentrations of water-soluble salts containing K and Na decrease, leading to a less reactive char during gasification [108]. Demineralization is known to increase the activation energy of feedstocks and concurrently decrease the maximum mass loss rates. This leads to an increase in the corresponding temperatures and a decrease in catalytic reactivity [109]. The demineralization of biomass with deionized water or acid is an effective way to remove AAEMs from biomass, leading to the improvement of feedstock decomposition [9,110]. However, demineralization using acidic or aqueous treatment has a different impact on the structure of the solid char with respect to its porosity and, thus, the available surface for the gasification reaction [111]. Demineralization has been performed using different leaching agents such as deionized water [9], acetic acid [112], hydrochloric acid [113], sulfuric acid [114,115], hydrofluoric acid [116], and nitric acid [117]. The difficulty of removing water-insoluble AAEMs has been reported in the literature [118]. Acid-based demineralization has shown a higher removal efficiency for both water-soluble and water-insoluble AAEMs [117]. However, some acid-soluble hydrocarbons, hemicellulose, and cellulose constituents, could be leached away during

the pre-treatment [119], which might create a competitive environment for the reactions caused by the organic and inorganic matter in the gasification and impact the formation of char [112]. Feedstock demineralization is an effective method to study the role of inherent or added inorganics on the composition and structure of gasification products, but due to the absence of a standard procedure for the feed demineralization, disputable results can be expected [56,120]. The addition of water-insoluble dolomite was found to have a negligible impact on the decomposition of hemicelluloses and cellulose, with consequently no impact on the gasification reactivity [121]. By contrast, investigations into the impact of Ca acetate on the devolatilization of cotton fibres and pure cellulose showed that Ca^{2+} ions inhibited the decomposition of both feedstocks [122]. This emphasized the importance of inorganics interaction with the organic matrix of biomass. The effect of potassium chloride on the pyrolysis of Danish wheat straw was investigated previously [123]. This study showed that the added inorganic compounds did not affect the yields or the composition of the pyrolysis product as the inherent minerals in the straw did. These results mean that minerals presented in different forms show different and even contrary behaviours; it is thus necessary to investigate the catalytic role of different intrinsic metal ions in biomass pyrolysis. In addition, biomass demineralization can lead to the unpredicted removal of lignin and other organic compounds. This causes fewer PAH precursors to be formed during rapid pyrolysis, and concurrently leads to lower yields of soot [34,124]. However, the unpredicted removal of lignin and other organic compounds did not have a strong impact on the char reactivity in further gasification experiments, causing only a negligible shift in the maximal reaction temperature towards less reactive char. The supercritical CO_2 extraction ($scCO_2$) has been less often investigated as a pre-treatment method for biomass gasification. The literature reports that the inorganic composition of wood after $scCO_2$ extraction remained unchanged [39]. However, $scCO_2$ is known to change the composition and concentrations of Mg^+, Si^+, and Ca^+ on the wood surface, which could potentially have an impact on the gasification reactivity [125]. The formation of a CaO-based thin layer on the char has been shown to increase graphitization and decrease reactivity during entrained-flow gasification at temperatures above 1000 °C [126]. More research is required to understand the impact of extraction on the physical properties and gasification reactivity of biomass.

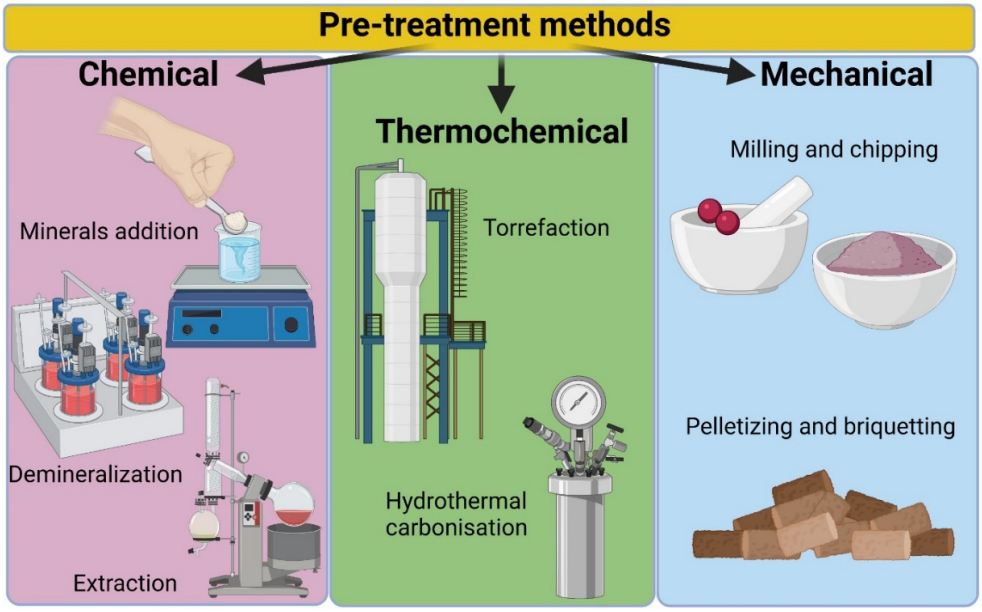

Figure 8. Pre-treatment methods which are related to the biomass gasification reactivity.

Thermochemical pre-treatment such as torrefaction is known to have an impact on the distribution of Ca, Mg, and Mn, with small changes in water-soluble K [127–129]. However,

the transformations in the inorganic matter composition are relatively small in torrefaction and thus have less influence on the CO_2 reactivity of torrefied feedstocks in TGA [130,131]. In addition, TGA results showed that both the inorganic matter and the lignocellulosic composition of olive stones had an equally small impact on the intrinsic reactivity of torrefied material in the further combustion or gasification stages [132]. The differences in the mineral content of the non-treated biomass prior to the hydrothermal carbonization (HTC) treatment determine the impact on the hydro-char gasification reactivity [133,134]. The HTC treatment of olive stones with an inorganic element content less than 2 wt.% had a negligible impact on the gasification reactivity due to the lower number of changes in the composition compared to the non-treated feedstock [132]. The high-ash banana leaves (9.2 wt.%) showed a decrease in K and Na content during HTC treatment, leading to the lower reactivity of hydro-char in the following thermogravimetric gasification compared to the non-treated banana leaves [135].

Mechanical pre-treatment such as milling can also have an impact on the gasification reactivity through the higher ash content in smaller biomass particles than in larger particle size fractions [131]. Small particles arising from the breakage of brittle large particles which are rich in inorganic matter are known to have a high inorganics content [112]. Thus, inorganics-rich small olive stone particles can cause a faster decomposition of feedstocks with the concurrent suppression of tars. This promotes higher yields of solid products and a higher CO_2 reactivity of char samples compared to ash lean chars [97]. The torrefied biomass particles of 0.18–0.425 mm in size have been previously shown to have an Ca content 50% greater than that of the 2–3 mm torrefied particles processed in the temperature range from 270 to 300 °C [132]. Small-sized torrefied biomass particles with higher Ca contents were also found to have almost double CO_2 reactivity in the further thermogravimetric analysis, emphasizing the impact of milling on the char properties. The literature does not report any clear correlation between mechanical pre-treatment methods and the impact of particle shape on the gasification reactivity. However, the wheat straw chars are known to obtain different shapes in pyrolysis, from near-spherical to cylindrical, due to the allocation of alkali metals in the original feedstock [97]. The formation of less fluid char from the pyrolysis of wheat straw was ascribed to stronger cross-linking reactions of herbaceous feedstocks under the catalytic effect of potassium and to a minor extent calcium [34]. The shape of the rice husk particles was cylindrical, and this did not significantly change during high-temperature treatment. This is probably due to the low softening temperature of amorphous silicon oxides (~700 °C) and the rapid cooling rate of char particles [97,136]. Thus, wheat straw particles are a mixture of various shapes due to the heterogenous distribution of alkali metals in the char matrix, leading to different surface area/volume ratios [137]. Cylindrical and flat particles of sizes $\geq$ 10 mm are less thick and have larger surface areas. This can result in a faster heat and mass transfer of CO_2 to the particle, leading to higher reactivity compared to the gasification of spherical char particles [138]. Small char particles with respect to the gasification reactivity are less sensitive to shape than are larger particles of the same material [139]. The briquetting and pelletizing processes are known to have a negligible impact on the char reactivity because the addition of quartz particles during the mixing with starch binders is the only reported way to change the inorganic composition of char samples [37].

3.7. Effect of Inherent Inorganic Content on Biomass Gasification

Table 4 reports the experimental studies that investigated the effect of inherent inorganic content on the gasification of raw or treated biomass. These studies directly subjected the biomass to gasification in TGA or a reactor, without having a separate char production step. Unlike char gasification studies that are often studied in TGA under steam or CO_2, biomass gasification has mostly been studied in gasifiers or reactors that include air as one of the gasifying agents. As discussed earlier, the residence time and temperature in gasification have a strong impact on reactivity. Hence, there may be some differences in the mechanisms and the overall reactivity effect in the case of raw biomass, primarily because

of the impact of volatiles released during the pyrolysis stage. However, most of the observations with respect to individual inorganic species are similar to those which were reported in char gasification studies. Some studies reported an interaction between different biomass organic components (cellulose/lignin) and AAEMs as influencing reactivity. For example, a higher cellulose content was held responsible for the prolonged gasification time and elevated peak temperature observed during CO_2 gasification [119].

Alkali metals influence the thermal decomposition mechanism during biomass gasification by enhancing the fragmentation (ring scission) of the monomers making up the macropolymer chains, leading to an increase in reactivity [140]. Steam gasification of rice husks and straw led to an enhancement of the heterogeneous char gasification reaction, the steam-tar reforming homogeneous H_2O–gas shift, and the hydrocarbon reforming reactions because of the AAEMs. Solid AAEMs existing in chars promoted heterogeneous reactions, whereas the volatilized AAEMs promoted homogeneous reactions [141]. It was also observed that the presence of external steam had no significant effect on the reforming of tars compared to AAEMs, but both factors did contribute to the improvement of the H_2/CO ratio of the syngas.

For fluidized-bed reactors, both the bed material and the fuel ash showed catalytic effects on biomass gasification. Fürsatz et al. reported a lower catalytic activity for pure K-Feldspar and olivine than limestone for water–gas shift reactions in a steam gasification set-up [142]. Limestone can be used as a bed material in fluidized-bed gasification. Furthermore, the results achieved with limestone can also be used as an indicator for long-term operation with high Ca-contents derived from biomass ash. As described above, CaO is enriched on the bed material surface during ash layer formation and the current state of knowledge in the field suggests its role as an active site on the particle surface with regards to char gasification or tar reforming [103]. For the steam gasification of coconut shells (CS), oil palms shells (OPS), and bamboo guadua (BG) in fluidized-bed reactors [143], inorganic content significantly influenced the gasification reactivity and kinetics over the lignocellulosic composition. The authors proposed a kinetic equation with the inorganic ratio term of K/(Si + P), which applied to a wide range of inorganic content, and H/C and O/C ratios near 1.5 and 0.8, respectively. Within the prescribed range, the equation could also predict the co-gasification behaviour of biomasses from the inorganic composition of each individual biomass. A study on fixed-bed gasification using wood with a lower composition in each inorganic element (<1.5%) reported better-quality syngas compared to gasification using inorganics-rich feedstock (>10%) [144]. When the same reactor was used for the co-gasification of high-ash biomass (~23% ash) and coal (~33% ash), a synergistic effect was obtained for the biomass-to-coal-blend ratio of 0.75 [145]. The effect was attributed to a trade-off between the catalytic effect of potassium and the inhibiting effect of alumina and silica, as well as to their proportions in the individual feedstock such as softwood and chicken manure.

Table 4. Experimental studies investigating the effects of inherent inorganic content on the gasification of raw or treated biomass.

Ref.	Gasification System	Feedstock	Main Findings
[146]	Fluidized-bed reactor at 1 atm, 800 °C in air at ER ~0.3	Bagasse and banana grass samples	Gas-phase inorganic species had K, Na, and Ca at concentration levels higher than specified for combustion turbine fuel, along with Si, Fe, P, and Cl. Bed material composition influenced inorganic retention.
[147]	Pressurized TGA, 800–900 °C; 1, 5, 10 bar, 100%, 70%, 30% CO_2 and H_2O	Barks of pine, spruce, birch, aspen	Reactivity increased at high temperature, but ash sintering was observed. The formation of silicates resulted in reduced catalytic activity, the formation of less reactive products, and high sintering tendencies.

Table 4. *Cont.*

Ref.	Gasification System	Feedstock	Main Findings
[119]	TGA, heated at 15 °C/min from 25 to 1200 °C in CO_2 flow of 100 mL/min	Woody and agricultural biomass. 1 M H_2SO_4 wash	Interaction between organic components (cellulose/lignin) and AAEMs influences reactivity. Higher cellulose contents probably prolong gasification time and elevate the peak temperature during CO_2 gasification. Acid-washed biomass showed lower peak values.
[141]	Spout-fluidized-bed reactor, 900 °C in steam flow of 125 mL/min	Rice straw and rice husk (dried and pulverized)	Solid AAEMs existing in chars promoted heterogeneous reactions (char gasification), gaseous AAEMs vapored from biomass promoted homogeneous reactions (water–gas shift, reforming reactions).
[144]	Fixed-bed downdraft gasifier of 10–15 kg/h feed, 800 °C in air at ER ~0.2 to 0.35	Garden waste (GW) (dry leaf litter) pellets	Higher ER increased the combustion zone temperature, which increased clinker formation. Wood with much lower ash contents showed better syngas quality than GW pellets, which confirms the dependance of reactivity on factors other than ash content.
[143]	Fluidized-bed reactor, 20 °C/min to 750–850 °C in 15% to 90% H_2O in N_2, total flow 11.7 L/min for 1 to 3 h	Oil palm shells (OPS), coconut shells (CS), and bamboo guadua (BG)	CO and CO_2 desorption of gasification chars followed the order of CS < BG < OPS, for which the respective K/(Si + P) values of the raw biomass were 3.9, 0.2, and 0.17. For K/(Si + P) > 1, char AAEM (especially K) resulted in a higher surface area and O-containing functional groups.
[148]	Fixed-bed reactor in 1 kW furnace, 600, 700, 800 °C in different ratios of CO_2 and N_2	Pine sawdust raw and mixed with CaO	CaO absorbed CO_2 and decreased the overall production of CO_2 but increased the production of H_2. The highest H_2/CO ratio was detected at 700 °C for a 2:1 ratio of N_2:CO_2.
[142]	100 kW_{th} dual fluidized-bed (DFB) steam gasification system	Softwood, chicken manure, mixture of two	Bed material and fuel ash both have a catalytic effect on gasification, as reported for the water–gas shift reaction. Pure K-Feldspar and olivine showed lower catalytic activity. High limestone led to a positive WGS equilibrium deviation through the catalysis of WGS and other reactions.

3.8. Effect of Externally Added Inorganic Content on Char/Biomass Gasification

Attempts were made to impregnate a range of minerals, especially metallic ones, to further understand the chemistry and the effects of inorganic content on gasification to optimize the gasifier performance. Table 5 shows the experimental studies investigating the effects of externally added inorganic content on the gasification of raw biomass and char. A few studies reviewed the role of external catalysts, particularly inorganic matter, in biomass gasification and observed similar results for H_2O and CO_2 gasification; for instance, potassium, sodium, and calcium were found to be the most effective catalysts, and silica and alumina are the most effective inhibitors [149,150]. On the one hand, the impregnation of alkali-rich ash or metals improves syngas quality by reducing tar and methane, but on the other hand, it may cause sintering or agglomeration, resulting in reduced char reactivities [151,152]. Biomass with high ash content and high silica content can also form agglomerates and enhance sintering in fluidized-bed gasification [153]. Gupta et al. impregnated 0–40% (*w*/*w*) K_2CO_3 in the char of dry leaf litter and observed an increased gasification rate up to 20% loading (*w*/*w*) but no significant rise beyond that point, implying that a 20% (*w*/*w*) addition could be the optimum [68]. Zhang et al. also observed that calcium loading up to 3 wt.% in wet coffee grounds increased reactivity, but loading higher than 3 wt.% led to poor dispersion, with significant decreases in the external surface area of the catalyst [154]. Hence, it is important to control the loading amount of

alkali species as well as regulate the gasifier operation to avoid the agglomeration of ash. Different measures to avoid the softening and agglomeration of ash in a real gasifier are reported in the literature [12,144].

The morphology and structure of char affected by inorganic content also plays a role in tar reforming reactions in the gasifier. The H_2O and CO_2 gasifying agents can significantly affect the tar–char interactions. It can also indirectly influence the tar reforming through changing the char catalyst structure. An increasing concentration of H_2O and CO_2 is known to strengthen the formation of additional oxygen-containing functional groups [155]. The heterogeneous reforming mechanism of biomass tar over biochar as a catalyst in the presence of H_2O and CO_2 at 800 °C has been reported in the literature [100,155]. Inorganic species in different forms may have a different impact on the reactivity. As an example, carbonate showed a stronger catalytic effect than chloride and alkali for the same alkali metal [64]. Nanou et al. established that the enhancement of the gasification rate depends on the amount and composition of ash as well as its distribution among and inside the char particles [156]. The distribution of inorganic content will depend on the method of external addition. Char obtained from AAEM-impregnated pinewood reached 100% conversion during steam gasification at 900 s, whereas char obtained from AAEM-impregnated pinewood reached only 50% conversion at 900 s [156]. In another study, the impregnation of water-leached wood showed poor reactivity compared to doped char [75]. Thus, the impregnation with AAEM species may be recommended for char samples rather than raw or washed biomass to obtain more accurate results. Figure 9 shows the gasification rates of the non-treated Chinese fir samples and their chars, which were doped with Na, Ca, K, Fe, and Mg with a loading of 0.04 g g^{-1} and which further reacted under CO_2 gasification in the TGA [92].

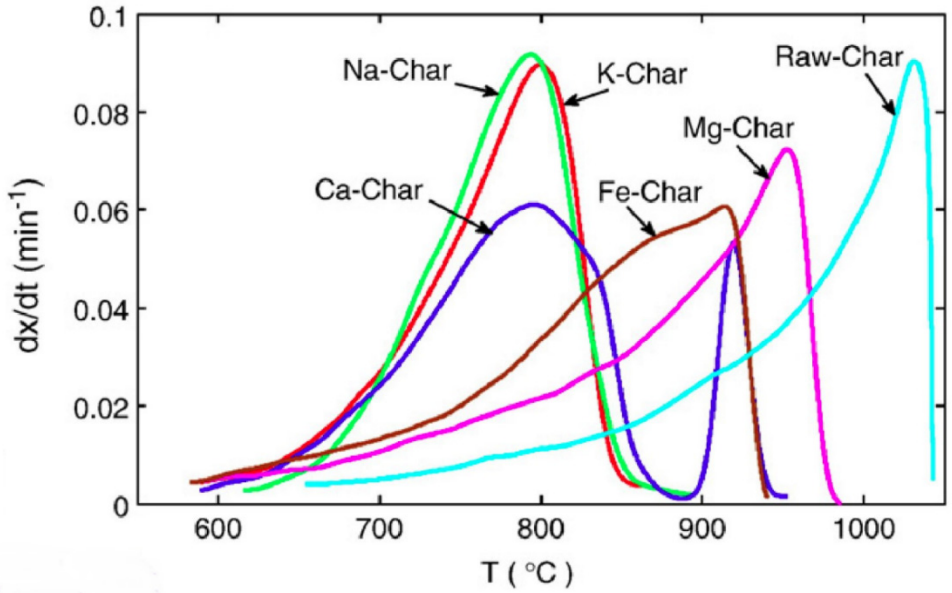

Figure 9. Gasification rates of different char samples with metal loading of 0.04 g/g [92].

The catalytic effects on the CO_2 gasification of biomass char decreased in the following order: K > Na > Ca > Fe > Mg. For Ca–char case, two peaks were detected in the gasification rate curve, in contrast to other char samples. The peak at the lower temperature (797 °C) represented the maximum of the Ca-catalysed reaction rate, while the peak at the higher temperature (919 °C) was the maximum of the uncatalysed reaction rate. The agglomeration and deactivation tendency of Ca at high temperatures is reported in gasification studies [149,157,158]. Vamvuka et al. impregnated $CaSO_4$ and various alkali bicarbonates into the organic fractions of municipal solid waste (MSW) to study the catalytic effect on CO_2 gasification at 950 °C [41]. For wastepaper gasification, the catalytic activity followed

the trend of Li_2CO_3 > K_2CO_3 > $CaCO_3$ > Rb_2CO_3 > $CaSO_4$ > Cs_2CO_3 > Na_2CO_3. For sewage sludge gasification, the trend was $CaCO_3$ > Na_2CO_3 > Li_2CO_3 > Rb_2CO_3 > $CaSO_4$ > Cs_2CO_3 > K_2CO_3. The difference in catalytic activities was attributed to different initial and intermediate compositions during gasification, and to the different molecular sizes and mobility on the carbon surface [41].

The dispersion and mobility of ash components are critical for their reactivity effects and vaporization at high temperatures. Bouraoui et al. observed a dispersion of impregnated K and Si in the char samples that was similar to that of natural K and Si but assumed a lower mobility of added K and Si than the natural ones [159,160]. Figure 10 shows the CO_2 gasification rates of beechwood char samples impregnated with different weight proportions of K and Si. In the case of Si impregnation, the effect was insignificant until 60% conversion, after which it showed an inhibitory effect [159]. In the case of K impregnation, after 40% conversion, the catalytic effect began to appear, which became more prominent towards higher conversions up to 90% [160]. For raw char with a K/Si ratio of 2, the CO_2 gasification reactivity increased up to 50% of conversion but decreased later because of the collapse of the pores or the deactivation of potential catalysts [159]. However, in the steam gasification of char with K/Si > 1, the reactivity was found to increase at higher conversions [72]. Figure 10 illustrates tests which were carried out with the same beechwood materials and using the same experimental procedures. This means that the reactivity effect of inorganic species is different in the presence of different gasifying agents. The discussion so far emphasizes the K/Si ratio as an important parameter for predicting gasification reactivity, particularly at higher conversions.

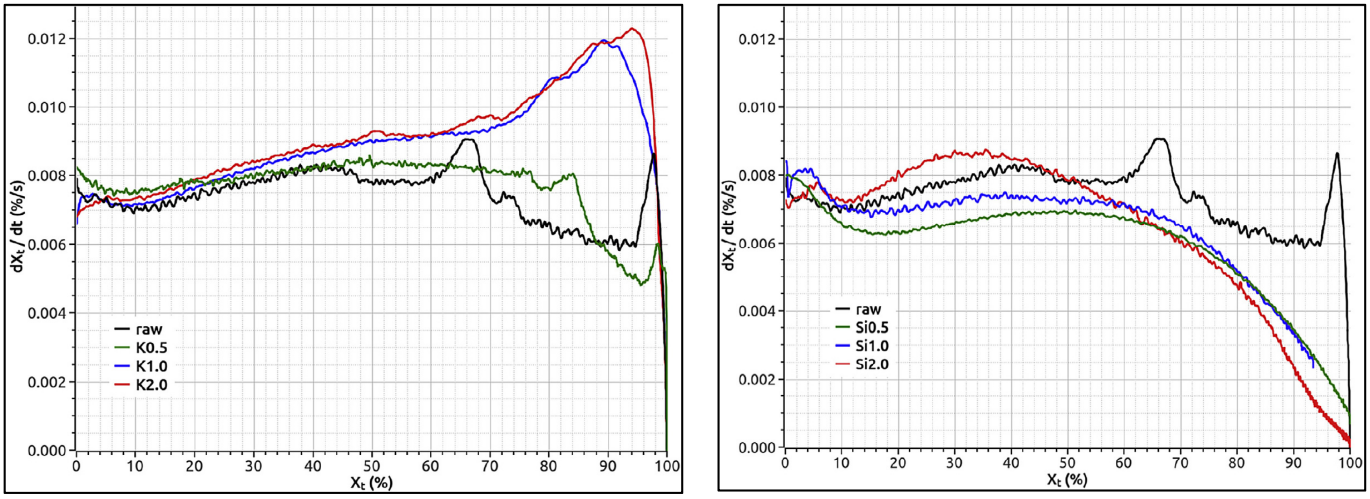

(**a**) (**b**)

Figure 10. CO_2 gasification rates of beechwood char samples impregnated with (**a**) K (0.5 wt.%, 1 wt.%, and 2 wt.%), and (**b**) Si (0.5 wt.%, 1 wt.%, and 2 wt.%) [159].

Table 5. Experimental studies investigating the effects of externally added inorganic content on gasification.

Ref.	Gasification System and Feedstock	Char Production	Main Findings
		Impregnated in biomass	
[151]	Fluidized-bed reactor, 2.4 atm, 700 °C H_2O/C (mol) = 1.1 Poplar wood mixed with 30% dry wood ash	TGA, 1 atm, 700–800 °C in N_2	The addition of alkali-rich ash to wood reduced tar and methane content and increased syngas production. However, alkali-rich ash can also form particle agglomerates.

Table 5. *Cont.*

Ref.	Gasification System and Feedstock	Char Production	Main Findings
		Impregnated in biomass	
[152]	TGA, 800 °C in CO_2 flow of 40 mL/min Wood, waste wood impregnated with 2 wt.% metal (Na, K, Ca, Mg, Cu, Pb, and Zn) nitrate solution	Fixed-bed reactor with pre-pyrolysis at 600 °C at 2.5 h and post-pyrolysis at 900 °C for 20 min in argon	A high catalytic activity was observed during the early gasification stage, but it was reduced in the next stage due to sintering. All heavy metal nitrate salts lowered the charcoal reactivity over the entire process.
[92]	TGA, 1 atm, 10 °C/min up to 1150 °C in CO_2 flow of 400 mL/min Chinese fir with metal loading 0.04 g/g	Quartz tube reactor, 5 °C/min until 550 °C, and held for 60 min in N_2 flow of 400 mL/min Wash: water	Catalytic effects on the CO_2 reactivity of char in the sequence of the most influencial to the least significant: K > Na > Ca > Fe > Mg. Ca tends to agglomerate and deactivate at high temperatures.
[32]	TGA, 1 atm, 10 °C/min to 950 °C, using CO_2 flow of 25 mL/min Municipal solid waste, undigested sewage sludge, paper External agent: $CaSO_4$ and various alkali bicarbonates (5–20% *w*/*w*)	TGA, 1 atm, 10 °C/min to 950 °C, in He flow	The difference in catalytic activities is due to different initial and intermediate compositions during gasification, and the different molecular sizes and mobility on the carbon surface. For waste paper gasification, activity: Li_2CO_3 > K_2CO_3 > $CaCO_3$ > Rb_2CO_3 > $CaSO_4$ > Cs_2CO_3 > Na_2CO_3 For sewage sludge gasification, activity: $CaCO_3$ > Na_2CO_3 > Li_2CO_3 > Rb_2CO_3 > $CaSO_4$ > Cs_2CO_3 > K_2CO_3.
[156]	TGA, 1 atm, 10 °C/min to 700 °C, in steam flow of 600 mL/min Pine wood and wheat straw External agent: Various salts of K, NaOH, CaO, Fe_2O_3	TGA, 1 atm, 10 °C/min to 700 °C, in N_2 flow of 600 mL/min	The enhancement of the gasification rate depends on the amount of ash as well as its distribution among and inside the char particles. For a metal/carbon ratio of 0.05 in wood, the catalytic activity trend was KNO_3 > $KHCO_3$ ≈ K_2CO_3 ≈ KOH > NaOH > CaO > K_2HPO_4 > KBr > KCl > no additive > Fe_2O_3.
[75]	Bubbling fluidized-bed reactor, 20% CO_2 and 80% N_2, gas velocity 0.2 m/s Raw and acid-washed birch wood External agent: Ca and K nitrate	Bubbling fluidized-bed reactor, using N_2, gas velocity 0.2 m/s External agent: Ca and K nitrate solutions	Leached wood showed poor reactivity upon doping compared to doped char. An unreactive coke layer developed over potassium-doped biomass chars, prohibiting K from the catalysis of char during gasification. Ca proved to be the primary active element in the gasification of birchwood.
[64]	Macro-TGA, 750–900 °C under CO_2 Pine sawdust External agent: 0.1 and 1 M K^+/Na^+ of salt solutions (K_2CO_3, Na_2CO_3, NaOH and NaCl)	Macro-TGA 600 °C for 4–5 min with the flow of CO_2 at 5 L/min, cooled down to room temperature by N_2	High metal loading altered char morphology. Reactivity was attributed to the combined effect of both organometallic bonds and alkali species, which were well dispersed on the surface. The enlarged surface area due to swelling and gasification temperature, and the final composition of alkali ions in chars, affect the reactivity.
		Impregnated in char	
[154]	TGA, 1 atm, 15 °C/min up to 800 °C in p_{CO2} = 0.1 MPa and p_{H2O} = 0.05 MPa in the argon flow of 450 mL/min, isothermal Wet coffee grounds	Infrared furnace, 600 °C/min to 900 °C, in argon flow of 200 mL/min for 1 min Ca loading during oil-slurry dewatering	Calcium loading up to 3 wt.% led to strong Ca dispersion into a biomass matrix and increased the reactivity, but with higher than 3 wt.% it led to poor dispersion with a significant decrease in the external surface area of the catalyst.

Table 5. *Cont.*

Ref.	Gasification System and Feedstock	Char Production	Main Findings
		Impregnated in char	
[161]	TGA, 1 atm, 10 °C/min to 850–950 °C, using CO_2 (20–80%) Japanese cypress	TGA, 9 °C/min to 850 °C, for 2 h in N_2 Wash: 3M HCl External agent: K_2CO_3 and $Ca(OH)_2$	The increase in CO_2 concentration increased the gasification rate of char at higher temperatures above 900 °C. At temperatures $\leq$ 850 °C, the gasification rate decreased at 80% CO_2 due to the inhibition effect of CO on alkali metal catalysts of carbon and CO_2.
[159]	TGA, 1 atm, 800 °C, using 80% N_2 and 20% CO_2 at 12 L/h Beechwood	TGA, 10 °C/min to 800 °C, in 25 L/h Ar External agent: KNO_3 and SiO_2	For impregnated char samples with a K/Si mass ratio from 0.2 to 3.8, the reactivity was same for all the samples until 60% conversion. Later, the effects of K and Si became evident, but for K/Si > 3, an acceleration in the gasification reaction was found at conversions $\geq$ 90%.
[68]	TGA 700–950 °C in CO_2 flow of 150 mL/min Jackfruit, mango, raintree, and eucalyptus leaf litter	Fixed-bed reactor at 10 °C/min to 800 °C in N_2 Wash: Water External agent: K_2CO_3 (0–40% *w*/*w*)	Char with a higher alkali index shows higher gasification reactivity. A modified random pore model with parameters incorporating the effect of inorganic species fitted the data for all biomass chars. The external addition of K_2CO_3 up to 20% loading (*w*/*w*) significantly increased the gasification rate.

3.9. Kinetics Models

The description of feedstock gasification requires a system to be simulated at its thermodynamic equilibrium, which can provide good results for the entrained-flow gasifiers. However, the fluidized-bed gasification system is known not to reach a state of equilibrium. Thus, kinetic modelling, despite its limitations, is used in the design of gasifiers.

The most commonly used kinetic models for biomass char gasification in steam or CO_2 are the volumetric model (VM), the shrinking core model (SCM) or grain model (GM), and the random pore model (RPM) [162].

$$\text{VM}: \frac{dx}{dt} = K(1-x) \tag{2}$$

$$\text{SCM}: \frac{dx}{dt} = K(1-x)^{3/2} \tag{3}$$

$$\text{RPM}: \frac{dx}{dt} = K(1-x)\sqrt{1-\psi \ln(1-x)} \tag{4}$$

where x is the conversion at time t, K denotes the reaction rate constant (min^{-1}), and ψ is a structural constant or shape factor.

In addition to these three models, the normal distribution function model (NDM) is another model based on the shape of the gasification rate curve [163].

$$\text{NDM}: \frac{dx}{dt} = r_m \exp\left(-\frac{(x-x_m)^2}{2\omega^2}\right) \tag{5}$$

where r_m is the gasification rate (min^{-1}), x_m is the conversion at maximum reactivity, and ω is the width of the curve at $r = r_m/2$.

These models, in their original form, are unable to explain the catalytic or inhibiting effect of inorganic content during biomass gasification. Hence, several modifications have been proposed for these models to account for these effects.

Table 6 shows different kinetic models having an additional factor to incorporate the effect of inorganic species on gasification reactivity.

Table 6. Different kinetic models incorporating the effect of inorganic species on gasification *.

Ref.	Model	System, Gasifying Agent, Feedstock
[150]	MRPM : $\frac{dx}{dt} = K(1-x)\sqrt{1-\psi\ln(1-x)}\left(1+(p+1)(bt)^p\right)$ where b is a constant of dimension [time^{-1}] and p is a dimensionless power law constant	TGA, CO_2, Fir charcoal
[60]	GM : $\frac{dx}{dt} = 87700\exp\left(\frac{-167000}{RT}\right)P_{H_2O}^{0.6}a_i(1-x)^{2/3}$ where $a_i = 0.1812\frac{m_K}{m_{Si}} + 0.5877$	TGA, H_2O, woody biomass
[67,68]	MRPM : $\frac{dx}{dt} = K(1-x)\sqrt{1-\psi\ln(1-x)}\left(1+(cx)^p\right)$ where c is a dimensionless constant, and p is a dimensionless power law constant	TGA, H_2O, CO_2, wood, herbaceous biomass
[162]	MSCM : $\frac{dx}{dt} = K(T)(1-x)^{2/3} + k_a x^{n_a}$ where k_a is the activation constant, and the activation order $n_a = 0.254[Ca] + 0.034$	TGA-MS, H_2O, Eucalyptus wood, fir wood, pine bark, lignin, cellulose, hemicellulose
[141]	ROM : $\frac{dx}{dt} = 13500\ \exp\left(\frac{-134000}{RT}\right)P_{H_2O}^{0.5}(1-x)^n k_1$ where P is the steam partial pressure, n is the theoretical model reaction order, and k_1 is the coefficient dependent on the ratio K/(Si + P)	TGA, H_2O, coconut shells, oil palm shells, bamboo guadua

* MRPM: modified random pore model; MSCM: modified shrinking core model; ROM: reaction order model; GM: grain model.

Di Blasi discusses the limitations of the kinetic models used in the gasification reactivity modelling [15]. The divergence in kinetic data due to the initial differences in char structure has a strong impact on the catalytic reactivity of inorganic matter and mass transfer limitations which can lead to variations in activation energy. Thus, the purer the carbon involved in feedstock decomposition, the more likely a higher activation energy becomes. This is due to the assumption about the presence of two parallel gasification reactions. The first reaction with a higher activation energy involves edge carbons, and the second one involves catalysed sites.

Almost all the modified models are semi-empirical in nature with no physical significance, and hence they may not be universally applicable even for a specific kind of biomass and a specific gasifying agent. For instance, a model developed for CO_2 gasification may not validate the experimental data for steam gasification of similar biomass. Moreover, these models do not account for the relation between the inorganic components and the lignocellulosic components of the biomass, as identified by some of the experimental studies discussed earlier. Hence, there is a need for developing a unified empirical model for a clear understanding of the catalytic or inhibitory effect of various inorganic species present in the biomass. The large number of available feedstocks in nature with various inorganic matter contents requires the development of a "universal" model.

4. Challenge and Future Research

Numerous investigations have been conducted on the effect of inorganic matter content on the gasification of non-treated feedstocks and char in TGA as well as reactors. There is a consensus on the catalytic effect of AAEMs, especially potassium, and the inhibitory effect of alumina and silica. However, a clear conclusion on the overall contribution of inorganic content to gasification reactivity in comparison to other factors is not available.

The effects of inorganic content are known but the underlying mechanisms are not yet clear. A few attempts have been made to understand the mechanism of the catalytic effect of potassium, but most of these studies lack the concrete experimental data to support the proposed mechanisms. Similarly for the inhibition effect of silica and alumina, a few FTIR-based analyses propose that the formation of metallic complexes and intermediates

dampens the catalytic effect of AAEMs and reduces the active sites and the porosity. There is a need for more experimental investigation at micro as well as macro scales with a sophisticated instrumental analysis of all the intermediates formed during the gasification process.

Co-gasification is looked upon as a potential process for treating diverse biomass with other solid feedstocks, after pre-treatment. The quantity and quality of the ash in the feedstocks can play a crucial role in selecting an appropriate blend ratio for co-gasification. There is a need to understand the role of inorganic content in various co-gasification examples, such as biomass-coal, biomass-petroleum, biomass-plastic, and biomass-sewage sludge blends. Co-gasification blends such as biomass-coal, torrefied biomass-char, or ash can balance the presence of alkali metals, leading to the development of a platform that controls the gasification reactivity. There is not yet a comprehensive understanding of the mechanisms underlying the reaction pathways for complex co-gasification mixtures. A first basis to understand the reaction pathways for inorganic components was postulated by Boström et al. based on woody biomass [164]. In this concept, the main ash transformation reactions were based on acid–base reaction probabilities. This concept shows the high degree of complexity when it comes to inorganic reactions using biomass. Further improvements were made by Skoglund, where a focus was placed on P-rich biomass fuels (either pure or in the form of fuel blends) [165]. When expanding this to co-gasification using biogenic residues from agriculture or food processing and waste streams from urban areas, the reaction pathways become significantly more complex. There is already a strong research focus on this topic, and it will become more important over the next years. Therefore, developments on the effects of inorganic components during the co-gasification of residues and waste needs to be regularly updated.

Most of the studies analysed the influence of inorganic content on gasifying agents such as CO_2 and H_2O. Many pilot-scale and commercial gasifiers operate using air or oxygen as gasifying agents. Hence, more studies are required to understand the role of inorganic content during air-blown/oxygen-brown gasification. Similarly, there is a need to extend such study to other oxygen carriers, such as metal oxides employed in chemical looping gasification.

More research is required to understand how to enhance or control the reactivity effects of inorganic content during gasification. The impregnation or mixing of catalytic elements in raw biomass as well as char helps to enhance the gasification reactions. The reactivity of solid chars in gasifiers can be controlled through demineralizing the biomass using water or acids. Some studies have proposed the addition of CO during gasification to inhibit alkali metal reduction, which opens another avenue for controlling reactivity in high-temperature processes and thus for addressing ash-related operational challenges in gasifiers.

Soot is another product of pyrolysis and gasification of biomass. The mechanism of alkali metal interaction with the soot and its impact on the reactivity has not been investigated very broadly. Thus, the present review emphasizes the importance of investigations related to the characterization of all solid products formed during pyrolysis and gasification to understand the impact of alkali metals on the reactivity.

There is a need for a kinetic model which is based on phenomenological parameters and which accounts for the effect of inorganic elements. Moreover, for inorganic species, the model should also consider the other compounds present in the ash in addition to K and Si. Inorganic content on the one hand can enhance the gasification performance, but on the other hand, it can also result in slag formation and/or agglomeration. This stresses the need for developing a strategy for the selection of appropriate feedstock, reactor, and the operating conditions. A "universal" model that will be valid for various operational conditions in gasification and individual feedstocks or blended species is needed in industrial and academic communities. The integration of predictive analytics using data analysis techniques such as artificial intelligence and machine learning may

contribute greatly to the development of a "universal" model to understand the interactions between inorganic matter and reactivity.

5. Conclusions

This review attempted to contribute to our understanding of the mechanisms involving K, Ca, and Si, with a particular focus on reaction kinetics. A knowledge of reaction mechanisms and kinetics in addition to the parameters on which they depend is important for reactor operation and design from the perspective of both process efficiency and environmental concern. Although the effects of inorganic content during gasification are known, the underlying mechanisms are not yet clear, which emphasizes the complexity of the ash transformation phenomena. More experimental investigations at micro and macro scales are suggested to control the reactivity effects of inorganic content during gasification including impregnation or the mixing of catalytic elements in raw biomass. Moreover, future studies on interactions between inorganic matter and gasification reactivity should include more investigations of the entire broad range of inorganic elements with the corresponding reaction kinetics.

Funding: This research received no external funding.

Acknowledgments: The author would like to thank the support of Björn Wahlströms and Jernkontoret Stiftelsen. The BioRender.com company is acknowledged for technical support and design of the figures. Sonal Thengane from the Indian Institute of Technology (IIT) Roorkee is acknowledged for consultancy during this review study.

Conflicts of Interest: The author declares no conflict of interest.

Appendix A

Table A1. Biomass pyrolysis and gasification reactions.

Biomass Pyrolysis Reactions [166]			
Primary reaction		Secondary reaction	
		Homogeneous (tar cracking)	Heterogeneous (tar–char reaction)
Raw biomass → Char (c_p) + Tar (tr) + Non-condensable gas (g_p)		Tar (tr) → Char (c_{s1}) + Non-condensable gas (g_{s1})	Tar (tr) + Char (c_p, c_{s1}, c_{s2}) → Char (c_{s2}) + Non-condensable gas (g_{s2})
Biomass Gasification Reactions [167]			
No.	**Description**	**Equation**	**ΔH (KJ/mole)**
1	Drying and Devolatilization	Biomass $\rightarrow C + \text{volatiles} + \text{ash} + H_2O$	>0
2	Partial oxidation	$C + 1/2O_2 \rightarrow CO$	−111
3	Complete oxidation	$C + O_2 \rightarrow CO_2$	−394
4	Boudouard reaction/CO_2 gasification	$C + CO_2 \rightarrow 2CO$	+173
5	Water gas reaction/Steam gasification	$C + H_2O \rightarrow CO + H_2$	+131
6	Hydrogen gasification	$C + 2H_2 \rightarrow CH_4$	−75
7	CO oxidation	$CO + 1/2O_2 \rightarrow CO_2$	−283
8	H_2 oxidation	$H_2 + 1/2O_2 \rightarrow H_2O$	−242
9	Methane oxidation	$CH_4 + 2O_2 \rightarrow CO_2 + 2H_2O$	−283
10	Water gas shift reaction	$CO + H_2O \leftrightarrow CO_2 + H_2$	−42
11	Methanation reaction	$CO + 3H_2 \rightarrow CH_4 + H_2O$	−88
12	Tar (C_xH_y) reactions	$C_xH_y + (O_2, CO_2, H_2) \rightarrow CO + CO_2 + CH_4 + H_2 + C$	+200 to 300

Appendix B

Table A2. Types of pyrolysis with primary distinguishing parameters.

Types	Residence Time	Temperature (°C)	Heating Rate	Desired Products
Slow	days	400	Very low	Charcoal
Intermediate	5–30 min	600	Low	Char, bio-oil, gas
Fast	<2 s	500	Very high	Bio-oil
Flash	<1 s	1000	High	Bio-oil, chemicals, gas
Vacuum	2–30 s	400	Medium	Bio-oil
Hydro-pyrolysis	<10 s	<500	High	Bio-oil
Under pressure	2–30 s	400	High	Bio-oil

Appendix C

Table A3. Experimental studies investigating the effects of inorganic content on the pyrolysis of raw and washed biomass.

Ref.	Equipment and Feedstock	Operating Conditions	Main Findings
		Inherent inorganic content	
[8]	Fluidized-bed reactor Switchgrass	500 °C, N_2, vapour residence time < 0.4 s, 0.34 mm particle size	Alkali metals in the char contribute to the mineral content of the bio-oil. For chlorine, nitrogen, and sulfur, there is only partial sequestration in the char particles.
[9]	Bubbling fluidized-bed reactor Willow, reed canary grass, switchgrass, wheat straw, and low lignin-containing grasses	150 g/h feed, 500 °C, N_2, vapor residence time 0.4–1.5 s	Total liquid yield (wt.%) increased with an increase in lignin, while the ash and alkali metal content decreased. Alkali metals lowered biomass degradation temperatures. Ash dominated over the lignin effect on pyrolysis yields, but lignin governed the higher-molecular-weight compounds in bio-oil.
[166]	Fixed-bed reactor Raw rice straw (RS), water-washed rice straw (WRS), and acid-washed rice straw (ARS)	2.2 g sample heated in argon (300 mL/min) at 10 °C/min to (275–725 °C)	Internal AAEMs and the changed organic matter influence the pyrolysis product distribution. Internal AAEMs act as catalysts for the decomposition of hemicellulose, cellulose, and lignin in raw RS.
[88]	Quartz fixed-bed reactor Maize stalk, rice husk, cotton stalk	At 900 °C the feedstock is pushed into the furnace, N_2, 10–300 s	Over half of the alkali metals (K, Na) were released during pyrolysis at 900 °C. Maize stalk char had a larger pore volume and superficial area than rice husks and cotton stalk char samples, indicating that the distinct reactivity of chars depends on the composition and distribution of the alkali metals released and those left in the char matrix.
[57]	Fluidized-bed reactor Pine wood (raw and acid-washed)	150 g biomass fed during 30–40 min, 530 °C, vapor residence time 1.6–1.9 s, feed particle average size of 1 mm	Acid washing reduced the yields of lignin-derived water insoluble content and guaiacol, due to the effect of mineral content on the decomposition behaviour of the lignin.

Table A3. *Cont.*

Ref.	Equipment and Feedstock	Operating Conditions	Main Findings
		Impregnated inorganic content	
[168]	Fixed-bed reactor and TGA 13 woody and herbaceous biomasses (raw and impregnated with metal chloride salt)	Reactor: 500 °C, 10–25 g sample in a batch reactor TGA: 50 °C/min, N_2	Devolatilization rate, volatiles yield, and the initial decomposition temperature increased upon demineralization for most biomasses. However, rice husk, groundnut shell, and coir pith showed different behaviour because of a high potassium (and/or zinc) content in combination with a high lignin content.
[121]	TGA Cellulose, hemicellulose, and lignin (raw and mixed with metal oxides and carbonates)	~20 mg sample heated at 10 °C/min up to 900 °C and kept for 3 min, N_2 flow 120 mL/min	The addition of K_2CO_3 inhibited hemicellulose pyrolysis but enhanced cellulose pyrolysis significantly by shifting its peak to a lower temperature. The assumed addition of K_2CO_3 changes the chemical structure of hemicellulose or the decomposition steps of cellulose.
[169]	TGA Pine wood, cotton stalk, fir (raw and treated with sodium-based catalysts, TiO_2 and HZSM-5)	10 mg sample heated at 10 °C/min, N_2 flow 100 mL/min	The devolatilization temperature was reduced with the increasing basicity of sodium-containing species. Sodium catalysts caused pyrolysis to be more exothermic and promoted char formation. TiO_2 and HZSM-5 increased the pyrolysis temperature of cotton stalk because the basic minerals were deactivated by the acidic nature of the catalysts.
[56]	TGA and analytical Py-GC/MS Poplar wood (demineralized with HF and impregnated with K, Ca, and Mg)	10 mg sample heated at 10 °C/min up to 700 °C	An increase in the potassium content of biomass increased char from 10.5 wt.% to 19.6 wt.% at 550 °C, and lowered the temperature of the maximum degradation rate from 367 °C to 333 °C. An increase in magnesium content increased the maximum degradation rate from 1.21 wt.%/°C to 1.43 wt.%/°C. K promoted the low-molecular-weight compounds and C6 and C2C6 lignin derivatives but suppressed levoglucosan.

References

1. Bruhn, T.; Naims, H.; Olfe-Kräutlein, B. Separating the debate on CO_2 utilisation from carbon capture and storage. *Environ. Sci. Policy* **2016**, *60*, 38–43. [CrossRef]
2. Thengane, S.K.; Bandyopadhyay, S. Biochar mines: Panacea to climate change and energy crisis? *Clean Technol. Environ. Policy* **2019**, *22*, 5–10. [CrossRef]
3. Sanchez, D.L.; Kammen, D.M. A commercialization strategy for carbon-negative energy. *Nat. Energy* **2016**, *1*, 15002. [CrossRef]
4. Akhtar, A.; Krepl, V.; Ivanova, T. A Combined Overview of Combustion, Pyrolysis, and Gasification of Biomass. *Energy Fuels* **2018**, *32*, 7294–7318. [CrossRef]
5. Heidenreich, S.; Foscolo, P.U. New concepts in biomass gasification. *Prog. Energy Combust. Sci.* **2015**, *46*, 72–95. [CrossRef]
6. Neves, D.; Thunman, H.; Matos, A.; Tarelho, L.; Gómez-Barea, A. Characterization and prediction of biomass pyrolysis products. *Prog. Energy Combust. Sci.* **2011**, *37*, 611–630. [CrossRef]
7. Sikarwar, V.; Zhao, M.; Fennell, P.S.; Shah, N.; Anthony, E.J. Progress in biofuel production from gasification. *Prog. Energy Combust. Sci.* **2017**, *61*, 189–248. [CrossRef]
8. Agblevor, F.A.; Besler, S. Inorganic Compounds in Biomass Feedstocks. 1. Effect on the Quality of Fast Pyrolysis Oils. *Energy Fuels* **1996**, *10*, 293–298. [CrossRef]
9. Fahmi, R.; Bridgwater, A.V.; Donnison, I.; Yates, N.; Jones, J.M. The effect of lignin and inorganic species in biomass on pyrolysis oil yields, quality and stability. *Fuel* **2008**, *87*, 1230–1240. [CrossRef]
10. Vassilev, S.V.; Baxter, D.; Vassileva, C.G. An overview of the behaviour of biomass during combustion: Part II. Ash fusion and ash formation mechanisms of biomass types. *Fuel* **2013**, *117*, 152–183. [CrossRef]
11. Herman, A.P.; Yusup, S.; Shahbaz, M.; Patrick, D.O. Bottom Ash Characterization and its Catalytic Potential in Biomass Gasification. *Procedia Eng.* **2016**, *148*, 432–436. [CrossRef]
12. James, A.K.; Thring, R.W.; Helle, S.; Ghuman, H.S. Ash Management Review—Applications of Biomass Bottom Ash. *Energies* **2012**, *5*, 3856–3873. [CrossRef]

13. Liu, Q. Pretreatment and Posttreatment Approaches for Reducing Biomass Inorganic Impurities during Gasification. Master's Thesis, University of Tennessee, Knoxville, TN, USA, 2017.
14. Risnes, H.; Fjellerup, J.; Henriksen, U.; Moilanen, A.; Norby, P.; Papadakis, K.; Posselt, D.; Sørensen, L.H. Calcium addition in straw gasification. *Fuel* **2003**, *82*, 641–651. [CrossRef]
15. Di Blasi, C. Combustion and gasification rates of lignocellulosic chars. *Prog. Energy Combust. Sci.* **2009**, *35*, 121–140. [CrossRef]
16. Dayton, D. *A Review of the Literature on Catalytic Biomass Tar Destruction*; National Renewable Energy Laboratory: Golden, CO, USA, 2002.
17. Gómez-Barea, A.; Ollero, P.; Leckner, B. Optimization of char and tar conversion in fluidized bed biomass gasifiers. *Fuel* **2013**, *103*, 42–52. [CrossRef]
18. Min, F.; Zhang, M.; Zhang, Y.; Cao, Y.; Pan, W.-P. An experimental investigation into the gasification reactivity and structure of agricultural waste chars. *J. Anal. Appl. Pyrolysis* **2011**, *92*, 250–257. [CrossRef]
19. Kannan, M.P.; Richards, G.N. Gasification of biomass chars in carbon dioxide: Dependence of gasification rate on the indigenous metal content. *Fuel* **1990**, *69*, 747–753. [CrossRef]
20. Okumura, Y.; Hanaoka, T.; Sakanishi, K. Effect of pyrolysis conditions on gasification reactivity of woody biomass-derived char. *Proc. Combust. Inst.* **2009**, *32*, 2013–2020. [CrossRef]
21. Giudicianni, P.; Gargiulo, V.; Grottola, C.M.; Alfè, M.; Ferreiro, A.I.; Mendes, M.A.A.; Fagnano, M.; Ragucci, R. Inherent Metal Elements in Biomass Pyrolysis: A Review. *Energy Fuels* **2021**, *35*, 5407–5478. [CrossRef]
22. Leijenhorst, E.J.; Wolters, W.; Van De Beld, L.; Prins, W. Inorganic element transfer from biomass to fast pyrolysis oil: Review and experiments. *Fuel Process. Technol.* **2016**, *149*, 96–111. [CrossRef]
23. Vassilev, S.V.; Vassileva, C.G.; Song, Y.-C.; Li, W.-Y.; Feng, J. Ash contents and ash-forming elements of biomass and their significance for solid biofuel combustion. *Fuel* **2017**, *208*, 377–409. [CrossRef]
24. Vassilev, S.V.; Baxter, D.; Andersen, L.K.; Vassileva, C.G.; Morgan, T.J. An overview of the organic and inorganic phase composition of biomass. *Fuel* **2011**, *94*, 1–33. [CrossRef]
25. Dahou, T.; Defoort, F.; Nguyen, H.N.; Bennici, S.; Jeguirim, M.; Dupont, C. Biomass steam gasification kinetics: Relative impact of char physical properties vs. inorganic composition. *Biomass-Convers. Biorefinery* **2020**, 1–16. [CrossRef]
26. Frandsen, F.J. *Ash Formation, Deposition and Corrosion when Utilizing Straw for Heat and Power Production*; DTU Chemical Engineering: Lyngby, Denmark, 2010.
27. De Jong, W.; Van Ommen, J.R. *Biomass as a Sustainable Energy Source for the Future: Fundamentals of Conversion Processes*; John Wiley & Sons, Inc.: New York, NY, USA, 2014; pp. 1–582. [CrossRef]
28. Kleinhans, U.; Wieland, C.; Frandsen, F.J.; Spliethoff, H. Ash formation and deposition in coal and biomass fired combustion systems: Progress and challenges in the field of ash particle sticking and rebound behavior. *Prog. Energy Combust. Sci.* **2018**, *68*, 65–168. [CrossRef]
29. Devi, T.G.; Kannan, M.P.; Abduraheem, V. Jump in the air gasification rate of potassium-doped cellulosic chars. *Fuel Process. Technol.* **2010**, *91*, 1826–1831. [CrossRef]
30. Surup, G.R.; Hunt, A.J.; Attard, T.; Budarin, V.L.; Forsberg, F.; Arshadi, M.; Abdelsayed, V.; Shekhawat, D.; Trubetskaya, A. The effect of wood composition and supercritical CO_2 extraction on charcoal production in ferroalloy industries. *Energy* **2019**, *193*, 116696. [CrossRef]
31. Trubetskaya, A.; Budarin, V.; Arshadi, M.; Magalhães, D.; Kazanç, F.; Hunt, A.J. Supercritical extraction of biomass as an effective pretreatment step for the char yield control in pyrolysis. *Renew. Energy* **2021**, *170*, 107–117. [CrossRef]
32. Lestander, T.A.; Lindeberg, J.; Eriksson, D.; Bergsten, U. Prediction of Pinus sylvestris clear-wood properties using NIR spectroscopy and biorthogonal partial least squares regression. *Can. J. For. Res.* **2008**, *38*, 2052–2062. [CrossRef]
33. Christensen, K.A.; Livbjerg, H. A Field Study of Submicron Particles from the Combustion of Straw. *Aerosol Sci. Technol.* **1996**, *25*, 185–199. [CrossRef]
34. Trubetskaya, A. Fast Pyrolysis of Biomass at HIGH Temperatures. Ph.D. Thesis, Technical University of Denmark, Lyngby, Denmark, 2016.
35. Ward, C.R. Analysis and significance of mineral matter in coal seams. *Int. J. Coal Geol.* **2002**, *50*, 135–168. [CrossRef]
36. Zevenhoven, M.; Yrjas, P.; Skrifvars, B.-J.; Hupa, M. Characterization of Ash-Forming Matter in Various Solid Fuels by Selective Leaching and Its Implications for Fluidized-Bed Combustion. *Energy Fuels* **2012**, *26*, 6366–6386. [CrossRef]
37. Trubetskaya, A.; Leahy, J.J.; Yazhenskikh, E.; Müller, M.; Layden, P.; Johnson, R.; Ståhl, K.; Monaghan, R.F. Characterization of woodstove briquettes from torrefied biomass and coal. *Energy* **2019**, *171*, 853–865. [CrossRef]
38. Llorente, M.J.F.; García, J.E.C. Concentration of elements in woody and herbaceous biomass as a function of the dry ashing temperature. *Fuel* **2006**, *85*, 1273–1279. [CrossRef]
39. Tolvanen, H. Advanced Solid Fuel Characterization for Reactivity and Physical Property Comparison. Ph.D. Thesis, Tampere University of Technology, Tampere, Finland, 2016.
40. Yao, M.; Wang, D.; Zhao, M. Element Analysis Based on Energy-Dispersive X-ray Fluorescence. *Adv. Mater. Sci. Eng.* **2015**, *2015*, 1–7. [CrossRef]
41. Vamvuka, D.; Karouki, E.; Sfakiotakis, S.; Salatino, P. Gasification of Waste Biomass Chars by Carbon Dioxide via Thermogravimetry—Effect of Catalysts. *Combust. Sci. Technol.* **2012**, *184*, 64–77. [CrossRef]

42. Limbeck, A.; Galler, P.; Bonta, M.; Bauer, G.; Nischkauer, W.; Vanhaecke, F. Recent advances in quantitative LA-ICP-MS analysis: Challenges and solutions in the life sciences and environmental chemistry ABC Highlights: Authored by Rising Stars and Top Experts. *Anal. Bioanal. Chem.* **2015**, *407*, 6593–6617. [CrossRef]
43. McComb, J.Q.; Rogers, C.; Han, F.X.; Tchounwou, P.B. Rapid Screening of Heavy Metals and Trace Elements in Environmental Samples Using Portable X-ray Fluorescence Spectrometer, A Comparative Study. *Water Air Soil Pollut.* **2014**, *225*, 1–10. [CrossRef]
44. Klug, H.P.; Alexander, L.E. *X-ray Diffraction Procedures for Polycrystalline and Amorphous Materials*, 2nd ed.; Wiley: New York, NY, USA, 1974; p. 992.
45. Ali, A.; Chiang, Y.W.; Santos, R.M. X-ray Diffraction Techniques for Mineral Characterization: A Review for Engineers of the Fundamentals, Applications, and Research Directions. *Minerals* **2022**, *12*, 205. [CrossRef]
46. Surup, G.R.; Nielsen, H.K.; Großarth, M.; Deike, R.; Van den Bulcke, J.; Kibleur, P.; Müller, M.; Ziegner, M.; Yazhenskikh, E. Effect of operating conditions and feedstock composition on the properties of manganese oxide or quartz charcoal pellets for the use in ferroalloy industries. *Energy* **2020**, *193*, 116736. [CrossRef]
47. Turpeinon, T. *Analysis of Microtomographic Images of Porous Heterogeneous Materials*; University of Jyväskylä: Jyväskylä, Finland, 2015.
48. Vanderesse, N.; Maire, E.; Chabod, A.; Buffière, J.-Y. Microtomographic study and finite element analysis of the porosity harmfulness in a cast aluminium alloy. *Int. J. Fatigue* **2011**, *33*, 1514–1525. [CrossRef]
49. Guntoro, P.I.; Ghorbani, Y.; Koch, P.-H.; Rosenkranz, J. X-ray Microcomputed Tomography (μCT) for Mineral Characterization: A Review of Data Analysis Methods. *Minerals* **2019**, *9*, 183. [CrossRef]
50. Bohlke, J.K.; Irwin, J. Laser microprobe analyses of Cl, Br, I, and K in fluid inclusions: Implications for sources of salinity in some ancient hydrothermal fluids. *Geochim. Cosmochim. Acta* **1992**, *56*, 203–225. [CrossRef]
51. Lanzetta, M.; Di Blasi, C. Pyrolysis kinetics of wheat and cornstraw. *J. Anal. Appl. Pyrolysis* **1998**, *44*, 181–192. [CrossRef]
52. Di Blasi, C. Modeling chemical and physical processes of wood and biomass pyrolysis. *Prog. Energy Combust. Sci.* **2008**, *34*, 47–90. [CrossRef]
53. Kuppens, T.; Van Dael, M.; Vanreppelen, K.; Carleer, R.; Yperman, J.; Schreurs, S.; Van Passel, S. Techno-economic assessment of pyrolysis char production and application a review. *Chem. Eng. Trans.* **2014**, *37*, 67–72. [CrossRef]
54. Bridgwater, A.V. Renewable fuels and chemicals by thermal processing of biomass. *Chem. Eng. J.* **2003**, *91*, 87–102. [CrossRef]
55. Grottola, C.M.; Giudicianni, P.; Pindozzi, S.; Stanzione, F.; Faugno, S.; Fagnano, M.; Fiorentino, N.; Ragucci, R. Steam assisted slow pyrolysis of contaminated biomasses: Effect of plant parts and process temperature on heavy metals fate. *Waste Manag.* **2019**, *85*, 232–241. [CrossRef]
56. Eom, I.-Y.; Kim, J.-Y.; Kim, T.-S.; Lee, S.-M.; Choi, D.; Choi, I.-G.; Choi, J.-W. Effect of essential inorganic metals on primary thermal degradation of lignocellulosic biomass. *Bioresour. Technol.* **2012**, *104*, 687–694. [CrossRef]
57. Oudenhoven, S.R.G.; Westerhof, R.J.M.; Aldenkamp, N.; Brilman, D.W.F.; Kersten, S.R.A. Demineralization of wood using wood-derived acid: Towards a selective pyrolysis process for fuel and chemicals production. *J. Anal. Appl. Pyrolysis* **2013**, *103*, 112–118. [CrossRef]
58. Ranzi, E.; Cuoci, A.; Faravelli, T.; Frassoldati, A.; Migliavacca, G.; Pierucci, S.; Sommariva, S. Chemical Kinetics of Biomass Pyrolysis. *Energy Fuels* **2008**, *22*, 4292–4300. [CrossRef]
59. Trubetskaya, A.; Surup, G.; Shapiro, A.; Bates, R.B. Modeling the influence of potassium content and heating rate on biomass pyrolysis. *Appl. Energy* **2017**, *194*, 199–211. [CrossRef]
60. Dupont, C.; Nocquet, T.; Da Costa, J.A.; Verne-Tournon, C. Kinetic modelling of steam gasification of various woody biomass chars: Influence of inorganic elements. *Bioresour. Technol.* **2011**, *102*, 9743–9748. [CrossRef] [PubMed]
61. Guizani, C.; Jeguirim, M.; Gadiou, R.; Escudero Sanz, F.J.; Salvador, S. Biomass char gasification by H_2O, CO_2 and their mixture: Evolution of chemical, textural and structural properties of the chars. *Energy* **2016**, *112*, 133–145. [CrossRef]
62. Liu, R.; Zhang, Y.; Ling, Z.; Song, Y. Some new insights into the synergy occurring during char gasification in CO_2/H_2O mixtures. *Fuel* **2020**, *268*, 117307. [CrossRef]
63. DeGroot, W.F.; Kannan, M.P.; Richards, G.N.; Theander, O. Gasification of agricultural residues (biomass): Influence of inorganic constituents. *J. Agric. Food Chem.* **1990**, *38*, 320–323. [CrossRef]
64. Kirtania, K.; Axelsson, J.; Matsakas, L.; Christakopoulos, P.; Umeki, K.; Furusjö, E. Kinetic study of catalytic gasification of wood char impregnated with different alkali salts. *Energy* **2017**, *118*, 1055–1065. [CrossRef]
65. Zhang, Y.; Wan, L.; Guan, J.; Xiong, Q.; Zhang, S.; Jin, X. A Review on Biomass Gasification: Effect of Main Parameters on Char Generation and Reaction. *Energy Fuels* **2020**, *34*, 13438–13455. [CrossRef]
66. Marquez-Montesinos, F.; Cordero, T.; Rodríguez-Mirasol, J.; Rodríguez, J. CO_2 and steam gasification of a grapefruit skin char. *Fuel* **2002**, *81*, 423–429. [CrossRef]
67. Dupont, C.; Boissonnet, G.; Seiler, J.-M.; Gauthier-Maradei, P.; Schweich, D. Study about the kinetic processes of biomass steam gasification. *Fuel* **2007**, *86*, 32–40. [CrossRef]
68. Gupta, A.; Thengane, S.K.; Mahajani, S. CO_2 gasification of char from lignocellulosic garden waste: Experimental and kinetic study. *Bioresour. Technol.* **2018**, *263*, 180–191. [CrossRef]
69. Kajita, M.; Kimura, T.; Norinaga, K.; Li, C.-Z.; Hayashi, J.-I. Catalytic and Noncatalytic Mechanisms in Steam Gasification of Char from the Pyrolysis of Biomass. *Energy Fuels* **2010**, *24*, 108–116. [CrossRef]

70. Zhu, W.; Song, W.; Lin, W. Catalytic gasification of char from co-pyrolysis of coal and biomass. *Fuel Process. Technol.* **2008**, *89*, 890–896. [CrossRef]
71. Lin, L.; Strand, M. Investigation of the intrinsic CO_2 gasification kinetics of biomass char at medium to high temperatures. *Appl. Energy* **2013**, *109*, 220–228. [CrossRef]
72. Hognon, C.; Dupont, C.; Grateau, M.; Delrue, F. Comparison of steam gasification reactivity of algal and lignocellulosic biomass: Influence of inorganic elements. *Bioresour. Technol.* **2014**, *164*, 347–353. [CrossRef]
73. Kirnbauer, F.; Wilk, V.; Kitzler, H.; Kern, S.; Hofbauer, H. The positive effects of bed material coating on tar reduction in a dual fluidized bed gasifier. *Fuel* **2012**, *95*, 553–562. [CrossRef]
74. Kuba, M.; Kraft, S.; Kirnbauer, F.; Maierhans, F.; Hofbauer, H. Influence of controlled handling of solid inorganic materials and design changes on the product gas quality in dual fluid bed gasification of woody biomass. *Appl. Energy* **2018**, *210*, 230–240. [CrossRef]
75. Kramb, J.; Gómez-barea, A.; Demartini, N.; Romar, H.; Rama, T.; Doddapaneni, K.C.; Konttinen, J. The effects of calcium and potassium on CO_2 gasification of birch wood in a fluidized bed. *Fuel* **2017**, *196*, 398–407. [CrossRef]
76. Knudsen, J.N.; Jensen, P.A.; Dam-Johansen, K. Transformation and Release to the Gas Phase of Cl, K, and S during Combustion of Annual Biomass. *Energy Fuels* **2004**, *18*, 1385–1399. [CrossRef]
77. Yip, K.; Tian, F.; Hayashi, J.-I.; Wu, H. Effect of Alkali and Alkaline Earth Metallic Species on Biochar Reactivity and Syngas Compositions during Steam Gasification†. *Energy Fuels* **2010**, *24*, 173–181. [CrossRef]
78. Ellis, N.; Masnadi, M.S.; Roberts, D.G.; Kochanek, M.A.; Ilyushechkin, A.Y. Mineral matter interactions during co-pyrolysis of coal and biomass and their impact on intrinsic char co-gasification reactivity. *Chem. Eng. J.* **2015**, *279*, 402–408. [CrossRef]
79. Matsumoto, K.; Takeno, K.; Ichinose, T.; Ogi, T.; Nakanishi, M. Gasification reaction kinetics on biomass char obtained as a by-product of gasification in an entrained-flow gasifier with steam and oxygen at 900–1000 °C. *Fuel* **2009**, *88*, 519–527. [CrossRef]
80. Johansen, J.M.; Jakobsen, J.G.; Frandsen, F.J.; Glarborg, P. Release of K, Cl, and S during Pyrolysis and Combustion of High-Chlorine Biomass. *Energy Fuels* **2011**, *25*, 4961–4971. [CrossRef]
81. Mermoud, F.; Salvador, S.; Vandesteene, L.; Golfier, F. Influence of the pyrolysis heating rate on the steam gasification rate of large wood char particles. *Fuel* **2006**, *85*, 1473–1482. [CrossRef]
82. Khalil, R.; Várhegyi, G.; Jäschke, S.; Grønli, M.G.; Hustad, J. CO_2 Gasification of Biomass Chars: A Kinetic Study. *Energy Fuels* **2008**, *23*, 94–100. [CrossRef]
83. Zhang, Y.; Geng, P.; Liu, R. Synergistic combination of biomass torrefaction and co-gasification: Reactivity studies. *Bioresour. Technol.* **2017**, *245*, 225–233. [CrossRef]
84. González-Vázquez, M.D.P.; García, R.; Gil, M.; Pevida, C.; Rubiera, F. Unconventional biomass fuels for steam gasification: Kinetic analysis and effect of ash composition on reactivity. *Energy* **2018**, *155*, 426–437. [CrossRef]
85. Ding, S.; Kantarelis, E.; Engvall, K. Effects of Porous Structure Development and Ash on the Steam Gasification Reactivity of Biochar Residues from a Commercial Gasifier at Different Temperatures. *Energies* **2020**, *13*, 5004. [CrossRef]
86. Dahou, T.; Defoort, F.; Khiari, B.; Labaki, M.; Dupont, C.; Jeguirim, M. Role of inorganics on the biomass char gasification reactivity: A review involving reaction mechanisms and kinetics models. *Renew. Sustain. Energy Rev.* **2020**, *135*, 110136. [CrossRef]
87. Ahmed, I.I.; Gupta, A.K. Kinetics of woodchips char gasification with steam and carbon dioxide. *Appl. Energy* **2011**, *88*, 1613–1619. [CrossRef]
88. Long, J.; Song, H.; Jun, X.; Sheng, S.; Lun-Shi, S.; Kai, X.; Yao, Y. Release characteristics of alkali and alkaline earth metallic species during biomass pyrolysis and steam gasification process. *Bioresour. Technol.* **2012**, *116*, 278–284. [CrossRef]
89. Mckee, D.W. Gasification of graphite in CO_2 and water vapor- the catalytic effect of metal salts. *Carbon N. Y.* **1982**, *20*, 59–66. [CrossRef]
90. Moulijn, J.A.; Cerfontain, M.B.; Kapteijn, F. Mechanism of the potassium catalysed gasification of carbon in CO_2. *Fuel* **1984**, *63*, 1043–1047. [CrossRef]
91. Masnadi, M.S.; Grace, J.R.; Bi, X.T.; Ellis, N.; Lim, C.J.; Butler, J.W. Biomass/coal steam co-gasification integrated with in-situ CO_2 capture. *Energy* **2015**, *83*, 326–336. [CrossRef]
92. Huang, Y.; Yin, X.; Wu, C.; Wang, C.; Xie, J.; Zhou, Z.; Ma, L.; Li, H. Effects of metal catalysts on CO_2 gasification reactivity of biomass char. *Biotechnol. Adv.* **2009**, *27*, 568–572. [CrossRef] [PubMed]
93. Hashimoto, K.; Miura, K.; Xu, J.-J.; Watanabe, A.; Masukami, H. Relation between the gasification rate of carbons supporting alkali metal salts and the amount of oxygen trapped by the metal. *Fuel* **1986**, *65*, 489–494. [CrossRef]
94. Duman, G.; Uddin, M.A.; Yanik, J. The effect of char properties on gasification reactivity. *Fuel Process. Technol.* **2014**, *118*, 32–40. [CrossRef]
95. Strandberg, A.; Holmgren, P.; Wagner, D.R.; Molinder, R.; Wiinikka, H.; Umeki, K.; Broström, M. Effects of Pyrolysis Conditions and Ash Formation on Gasification Rates of Biomass Char. *Energy Fuels* **2017**, *31*, 6507–6514. [CrossRef]
96. Strandberg, A. Fuel Conversion and Ash Formation Interactions A Thermochemical Study on Lignocellulosic Biomass. Ph.D. Thesis, Umeå University, Umeå, Sweden, 2018.
97. Trubetskaya, A.; Jensen, P.A.; Jensen, A.D.; Steibel, M.; Spliethoff, H.; Glarborg, P.; Larsen, F.H. Comparison of high temperature chars of wheat straw and rice husk with respect to chemistry, morphology and reactivity. *Biomass-Bioenergy* **2016**, *86*, 76–87. [CrossRef]

98. Novaković, A.; van Lith, S.C.; Frandsen, F.J.; Jensen, P.A.; Holgersen, L.B. Release of Potassium from the Systems K−Ca−Si and K−Ca−P. *Energy Fuels* **2009**, *23*, 3423–3428. [CrossRef]
99. Zhang, Z.; Song, Q.; Yao, Q.; Yang, R. Influence of the Atmosphere on the Transformation of Alkali and Alkaline Earth Metallic Species during Rice Straw Thermal Conversion. *Energy Fuels* **2012**, *26*, 1892–1899. [CrossRef]
100. Yu, J.; Guo, Q.; Gong, Y.; Ding, L.; Wang, J.; Yu, G. A review of the effects of alkali and alkaline earth metal species on biomass gasification. *Fuel Process. Technol.* **2021**, *214*, 106723. [CrossRef]
101. Trubetskaya, A.; Larsen, F.H.; Shchukarev, A.; Ståhl, K.; Umeki, K. Potassium and soot interaction in fast biomass pyrolysis at high temperatures. *Fuel* **2018**, *225*, 89–94. [CrossRef]
102. Vilches, T.B.; Maric, J.; Knutsson, P.; Rosenfeld, D.C.; Thunman, H.; Seemann, M. Bed material as a catalyst for char gasification: The case of ash-coated olivine activated by K and S addition. *Fuel* **2018**, *224*, 85–93. [CrossRef]
103. Larsson, A.; Kuba, M.; Vilches, T.B.; Seemann, M.; Hofbauer, H.; Thunman, H. Steam gasification of biomass—Typical gas quality and operational strategies derived from industrial-scale plants. *Fuel Process. Technol.* **2020**, *212*, 106609. [CrossRef]
104. Kuba, M.; Fürsatz, K.; Janisch, D.; Aziaba, K.; Chlebda, D.; Łojewska, J.; Forsberg, F.; Umeki, K.; Hofbauer, H. Surface characterization of ash-layered olivine from fluidized bed biomass gasification. *Biomass-Convers. Biorefinery* **2020**, *11*, 29–38. [CrossRef]
105. Kryca, J.; Priščák, J.; Łojewska, J.; Kuba, M.; Hofbauer, H. Apparent kinetics of the water-gas-shift reaction in biomass gasification using ash-layered olivine as catalyst. *Chem. Eng. J.* **2018**, *346*, 113–119. [CrossRef]
106. Benedikt, F.; Fuchs, J.; Schmid, J.C.; Müller, S.; Hofbauer, H. Advanced dual fluidized bed steam gasification of wood and lignite with calcite as bed material. *Korean J. Chem. Eng.* **2017**, *34*, 2548–2558. [CrossRef]
107. Kuba, M.; Skoglund, N.; Öhman, M.; Hofbauer, H. A review on bed material particle layer formation and its positive influence on the performance of thermo-chemical biomass conversion in fluidized beds. *Fuel* **2021**, *291*, 120214. [CrossRef]
108. Namkung, H.; Park, J.-H.; Lee, Y.-J.; Song, G.-S.; Choi, J.W.; Park, S.-J.; Kim, S.; Liu, J.; Choi, Y.-C. Performance evaluation of biomass pretreated by demineralization and torrefaction for ash deposition and PM emissions in the combustion experiments. *Fuel* **2021**, *292*, 120379. [CrossRef]
109. Zhao, D.; Dai, Y.; Chen, K.; Sun, Y.; Yang, F.; Chen, K. Effect of potassium inorganic and organic salts on the pyrolysis kinetics of cigarette paper. *J. Anal. Appl. Pyrolysis* **2013**, *102*, 114–123. [CrossRef]
110. Davidsson, K.O.; Korsgren, J.G.; Pettersson, J.B.C. The effects of fuel washing techniques on alkali release from biomass. *Fuel* **2002**, *81*, 137–142. [CrossRef]
111. Arnold, R.A.; Hill, J.M. Catalysts for gasification: A review. *Sustain. Energy Fuels* **2019**, *3*, 656–672. [CrossRef]
112. Liu, X.; Bi, X.T. Removal of inorganic constituents from pine barks and switchgrass. *Fuel Process. Technol.* **2011**, *92*, 1273–1279. [CrossRef]
113. Mayer, Z.A.; Apfelbacher, A.; Hornung, A. Effect of sample preparation on the thermal degradation of metal-added biomass. *J. Anal. Appl. Pyrolysis* **2012**, *94*, 170–176. [CrossRef]
114. Fierro, V.; Torné-Fernández, V.; Celzard, A.; Montané, D. Influence of the demineralisation on the chemical activation of Kraft lignin with orthophosphoric acid. *J. Hazard. Mater.* **2007**, *149*, 126–133. [CrossRef]
115. Keown, D.M.; Hayashi, J.-I.; Li, C.-Z. Effects of volatile–char interactions on the volatilisation of alkali and alkaline earth metallic species during the pyrolysis of biomass. *Fuel* **2008**, *87*, 1187–1194. [CrossRef]
116. Das, P.; Ganesh, A.; Wangikar, P. Influence of pretreatment for deashing of sugarcane bagasse on pyrolysis products. *Biomass-Bioenergy* **2004**, *27*, 445–457. [CrossRef]
117. Mourant, D.; Wang, Z.; He, M.; Wang, X.S.; Garcia-Perez, M.; Ling, K.; Li, C.-Z. Mallee wood fast pyrolysis: Effects of alkali and alkaline earth metallic species on the yield and composition of bio-oil. *Fuel* **2011**, *90*, 2915–2922. [CrossRef]
118. Tan, H.; Wang, S.-R. Experimental study of the effect of acid-washing pretreatment on biomass pyrolysis. *J. Fuel Chem. Technol.* **2009**, *37*, 668–672. [CrossRef]
119. Lv, D.; Xu, M.; Liu, X.; Zhan, Z.; Li, Z.; Yao, H. Effect of cellulose, lignin, alkali and alkaline earth metallic species on biomass pyrolysis and gasification. *Fuel Process. Technol.* **2010**, *91*, 903–909. [CrossRef]
120. Eom, I.-Y.; Kim, K.-H.; Kim, J.-Y.; Lee, S.-M.; Yeo, H.-M.; Choi, I.-G.; Choi, J.-W. Characterization of primary thermal degradation features of lignocellulosic biomass after removal of inorganic metals by diverse solvents. *Bioresour. Technol.* **2010**, *102*, 3437–3444. [CrossRef] [PubMed]
121. Yang, H.; Yan, R.; Chen, H.; Zheng, C.; Lee, D.H.; Liang, D.T. In-Depth Investigation of Biomass Pyrolysis Based on Three Major Components: Hemicellulose, Cellulose and Lignin. *Energy Fuels* **2006**, *20*, 388–393. [CrossRef]
122. Jakab, E.; Sebestyén, Z.; May, Z.; Réczey, K. The effect of alkaline pretreatment on the thermal decomposition of hemp. *J. Therm. Anal.* **2010**, *105*, 1061–1069. [CrossRef]
123. Jensen, A.; Dam-Johansen, K.; Wójtowicz, M.A.; Serio, M.A. TG-FTIR Study of the Influence of Potassium Chloride on Wheat Straw Pyrolysis. *Energy Fuels* **1998**, *12*, 929–938. [CrossRef]
124. Trubetskaya, A.; Jensen, P.A.; Jensen, A.D.; Llamas, A.D.G.; Umeki, K.; Glarborg, P. Effect of fast pyrolysis conditions on biomass solid residues at high temperatures. *Fuel Process. Technol.* **2016**, *143*, 118–129. [CrossRef]
125. Trubetskaya, A.; Budarin, V.; Arshadi, M.; Grams, J.; Hunt, A.J. Supercritical extraction of biomass Extraction of Biomass—A Green and Sustainable Method to Control the Pyrolysis Product Distirbution. *ACS Sustain. Chem. Eng.* **2021**, *9*, 5278–5287. [CrossRef]

126. Schneider, C.; Walker, S.; Phounglamcheik, A.; Umeki, K.; Kolb, T. Effect of calcium dispersion and graphitization during high-temperature pyrolysis of beech wood char on the gasification rate with CO_2. *Fuel* **2020**, *283*, 118826. [CrossRef]
127. Bajcar, M.; Zagula, G.; Saletnik, B.; Tarapatskyy, M.; Puchalski, C. Relationship between Torrefaction Parameters and Physicochemical Properties of Torrefied Products Obtained from Selected Plant Biomass. *Energies* **2018**, *11*, 2919. [CrossRef]
128. Li, T.; Geier, M.T.; Wang, L.; Shaddix, C.R.; Ku, X.; Matas Güell, B.; Lovås, T. Effect of Torrefaction on Physical Properties and Conversion Behavior of High Heating Rate Char of Forest Residue. *Energy Fuels* **2014**, *29*, 177–184. [CrossRef]
129. Shoulaifar, T.K.; DeMartini, N.; Zevenhoven, M.; Verhoeff, F.; Kiel, J.; Hupa, M. Ash-Forming Matter in Torrefied Birch Wood: Changes in Chemical Association. *Energy Fuels* **2013**, *27*, 5684–5690. [CrossRef]
130. Barta-Rajnai, E.; Jakab, E.; Sebestyén, Z.; May, Z.; Barta, Z.; Wang, L.; Skreiberg, Ø.; Grønli, M.; Bozi, J.; Czégény, Z. Comprehensive Compositional Study of Torrefied Wood and Herbaceous Materials by Chemical Analysis and Thermoanalytical Methods. *Energy Fuels* **2016**, *30*, 8019–8030. [CrossRef]
131. Branca, C.; Di Blasi, C.; Galgano, A.; Broström, M. Effects of the Torrefaction Conditions on the Fixed-Bed Pyrolysis of Norway Spruce. *Energy Fuels* **2014**, *28*, 5882–5891. [CrossRef]
132. Trubetskaya, A.; Leahy, J.J.; Grams, J.; Kwapinska, M.; Gallagher, P.; Johnson, R.; Monaghan, R.F.D. The effect of particle size, temperature and residence time on the yields and reactivity of olive stones from torrefaction. *Renew. Energy* **2020**, *160*, 998–1011. [CrossRef]
133. Surup, G.R.; Timko, M.T.; Leahy, J.J.; Trubetskaya, A. Hydrothermal carbonization of olive wastes to produce renewable, binder-free pellets for use as metallurgical reducing agents. *Renew. Energy* **2020**, *155*, 347–357. [CrossRef]
134. Mosqueda, A.; Medrano, K.; Gonzales, H.; Yoshikawa, K. Effect of hydrothermal and washing treatment of banana leaves on co-gasification reactivity with coal. *Energy Procedia* **2019**, *158*, 785–791. [CrossRef]
135. Hedler, A.; Klaumünzer, S.L.; Wesch, W. Amorphous silicon exhibits a glass transition. *Nat. Mater.* **2004**, *3*, 804–809. [CrossRef]
136. Momeni, M.; Yin, C.; Kær, S.K.; Hansen, T.B.; Jensen, P.A.; Glarborg, P. Experimental Study on Effects of Particle Shape and Operating Conditions on Combustion Characteristics of Single Biomass Particles. *Energy Fuels* **2012**, *27*, 507–514. [CrossRef]
137. Lu, H. Experimental and Modeling Investigations of Biomass Particle Combustion. Ph.D. Thesis, Brigham Young University, Provo, UT, USA, 2006.
138. Lu, H.; Ip, E.; Scott, J.; Foster, P.; Vickers, M.; Baxter, L.L. Effects of particle shape and size on devolatilization of biomass particle. *Fuel* **2010**, *89*, 1156–1168. [CrossRef]
139. Bhatia, S.K.; Perlmutter, D.D. A random pore model for fluid-solid reactions: I. Isothermal, kinetic control. *AIChE J.* **1980**, *26*, 379–386. [CrossRef]
140. Jiang, L.; Hu, S.; Wang, Y.; Su, S.; Sun, L.; Xu, B.; He, L.; Xiang, J. Catalytic effects of inherent alkali and alkaline earth metallic species on steam gasification of biomass. *Int. J. Hydrogen Energy* **2015**, *40*, 15460–15469. [CrossRef]
141. María, L.; Millán, R.; Emiro, F.; Vargas, S.; Nzihou, A. Steam gasification behavior of tropical agrowaste: A new modeling approach based on the inorganic composition. *Fuel* **2018**, *235*, 45–53. [CrossRef]
142. Fürsatz, K.; Fuchs, J.; Benedikt, F.; Kuba, M.; Hofbauer, H. Effect of biomass fuel ash and bed material on the product gas composition in DFB steam gasification. *Energy* **2020**, *219*, 119650. [CrossRef]
143. Millán, L.M.R.; Vargas, F.E.S.; Nzihou, A. Catalytic Effect of Inorganic Elements on Steam Gasification Biochar Properties from Agrowastes. *Energy Fuels* **2019**, *33*, 8666–8675. [CrossRef]
144. Siddiqui, H.; Thengane, S.K.; Sharma, S.; Mahajani, S.M. Revamping downdraft gasifier to minimize clinker formation for high-ash garden waste as feedstock. *Bioresour. Technol.* **2018**, *266*, 220–231. [CrossRef] [PubMed]
145. Thengane, S.K.; Gupta, A.; Mahajani, S.M. Co-gasification of high ash biomass and high ash coal in downdraft gasifier. *Bioresour. Technol.* **2018**, *273*, 159–168. [CrossRef] [PubMed]
146. Turn, S.Q.; Kinoshita, C.M.; Ishimura, D.M.; Zhou, J. The fate of inorganic constituents of biomass in fluidized bed gasification. *Fuel* **1998**, *77*, 135–146. [CrossRef]
147. Moilanen, A.; Nasrullah, M.; Kurkela, E. The effect of biomass feedstock type and process parameters on achieving the total carbon conversion in the large scale fluidized bed gasification of biomass. *Environ. Prog. Sustain. Energy* **2009**, *28*, 355–359. [CrossRef]
148. Gao, N.; Śliz, M.; Quan, C.; Bieniek, A.; Magdziarz, A. Biomass CO_2 gasification with CaO looping for syngas production in a fixed-bed reactor. *Renew. Energy* **2020**, *167*, 652–661. [CrossRef]
149. Nzihou, A.; Stanmore, B.; Sharrock, P. A review of catalysts for the gasification of biomass char, with some reference to coal. *Energy* **2013**, *58*, 305–317. [CrossRef]
150. Ong, H.C.; Chen, W.-H.; Farooq, A.; Gan, Y.Y.; Lee, K.T.; Ashokkumar, V. Catalytic thermochemical conversion of biomass for biofuel production: A comprehensive review. *Renew. Sustain. Energy Rev.* **2019**, *113*, 109266. [CrossRef]
151. Hauserman, W. High-yield hydrogen production by catalytic gasification of coal or biomass. *Int. J. Hydrogen Energy* **1994**, *19*, 413–419. [CrossRef]
152. Struis, R.P.W.J.; Von Scala, C.; Stucki, S.; Prins, R. Gasification reactivity of charcoal with CO_2. Part I: Conversion and structural phenomena. *Chem. Eng. Sci.* **2002**, *57*, 3581–3592. [CrossRef]
153. Moilanen, A.; Nasrullah, M. *Gasification Reactivity and Ash Sintering Behaviour of Biomass Feedstocks*; VTT Publications: Espoo, Finland, 1982.

154. Zhang, Y.; Ashizawa, M.; Kajitani, S. Calcium loading during the dewatering of wet biomass in kerosene and catalytic activity for subsequent char gasification. *Fuel* **2008**, *87*, 3024–3030. [CrossRef]
155. Feng, D.; Zhao, Y.; Zhang, Y.; Sun, S. Effects of H_2O and CO_2 on the homogeneous conversion and heterogeneous reforming of biomass tar over biochar. *Int. J. Hydrogen Energy* **2017**, *42*, 13070–13084. [CrossRef]
156. Nanou, P.; Murillo, H.E.G.; van Swaaij, W.P.; van Rossum, G.; Kersten, S.R. Intrinsic reactivity of biomass-derived char under steam gasification conditions-potential of wood ash as catalyst. *Chem. Eng. J.* **2013**, *217*, 289–299. [CrossRef]
157. Lee, D.; Kung, K.; Ratti, C. Mapping the Waste Handling Dynamics in Mombasa Using Mobile Phone GPS. In Proceedings of the 14th International Conference on Computers in Urban Planning and Urban Management, Cambridge, MA, USA, 7–10 July 2015.
158. Seemen, A.; Atong, D.; Sricharoenchaikul, V. Effect of Silica and Alumina Ratio on Bed Agglomeration during Fluidized Bed Gasification of Rice Straw. In Proceedings of the 2018 2nd International Conference on Green Energy and Applications (ICGEA), Singapore, 24–26 March 2018.
159. Bouraoui, Z.; Jeguirim, M.; Limousy, L.; Dupont, C.; Gadiou, R. CO_2 gasification of woody biomass chars: The influence of K and Si on char reactivity. *C. R. Chim.* **2016**, *19*, 457–465. [CrossRef]
160. Baxter, L.L.; Miles, T.R.; Miles, T.R.; Jenkins, B.M.; Milne, T.; Dayton, D.; Bryers, R.W.; Oden, L.L. The behavior of inorganic material in biomass-fired power boilers: Field and laboratory experiences. *Fuel Process. Technol.* **1998**, *54*, 47–78. [CrossRef]
161. Mitsuoka, K.; Hayashi, S.; Amano, H.; Kayahara, K.; Sasaoaka, E.; Uddin, A. Gasification of woody biomass char with CO_2: The catalytic effects of K and Ca species on char gasification reactivity. *Fuel Process. Technol.* **2011**, *92*, 26–31. [CrossRef]
162. López-González, D.; Fernandez-Lopez, M.; Valverde, J.L.; Sanchez-Silva, L. Gasification of lignocellulosic biomass char obtained from pyrolysis: Kinetic and evolved gas analyses. *Energy* **2014**, *71*, 456–467. [CrossRef]
163. Lahijani, P.; Alimuddin, Z.; Rahman, A.; Mohammadi, M. CO_2 gasification reactivity of biomass char: Catalytic influence of alkali, alkaline earth and transition metal salts. *Bioresour. Technol.* **2013**, *144*, 288–295. [CrossRef]
164. Boström, D.; Skoglund, N.; Grimm, A.; Boman, C.; Öhman, M.; Broström, M.; Backman, R. Ash Transformation Chemistry during Combustion of Biomass. *Energy Fuels* **2011**, *26*, 85–93. [CrossRef]
165. Skoglund, N. Ash Chemistry and Fuel Design Focusing on Combustion of Phosphorus-Rich Biomass. Ph.D. Thesis, Umeå University, Umeå, Sweden, 2014.
166. Shi, L.; Yu, S.; Wang, F.C.; Wang, J. Pyrolytic characteristics of rice straw and its constituents catalyzed by internal alkali and alkali earth metals. *Fuel* **2012**, *96*, 586–594. [CrossRef]
167. Gomez-Barea, A.; Leckner, B. Modeling of biomass gasification in fluidized bed. *Prog. Energy Combust. Sci.* **2010**, *36*, 444–509. [CrossRef]
168. Raveendran, K.; Ganesh, A.; Khilar, K.C. Influence of mineral matter on biomass pyrolysis characteristics. *Fuel* **1995**, *74*, 1812–1822. [CrossRef]
169. Wang, J.; Zhang, M.; Chen, M.; Min, F.; Zhang, S.; Ren, Z.; Yan, Y. Catalytic effects of six inorganic compounds on pyrolysis of three kinds of biomass. *Thermochim. Acta* **2006**, *444*, 110–114. [CrossRef]